NATIONAL ADVISORY COMMITTEE FOR AERONAUTICS

TECHNICAL NOTE

No. 1002

STRESS ANALYSIS OF COLUMNS AND BEAM COLUMNS

BY THE PHOTOELASTIC METHOD
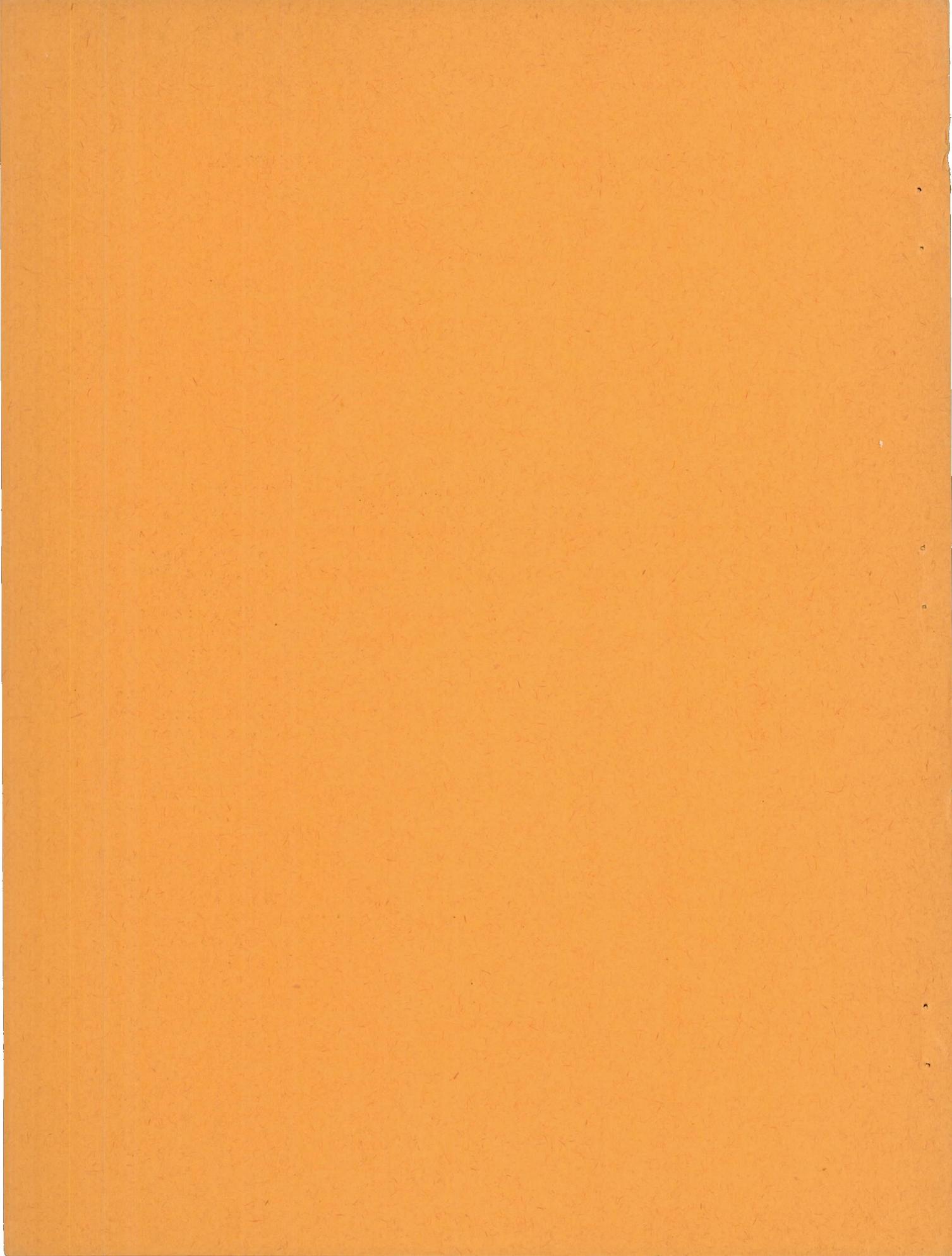
By B. F. Ruffner
Oregon State College

NACA

Washington
March 1946

NATIONAL ADVISORY COMMITTEE FOR AERONAUTICS

———————

TECHNICAL NOTE NO. 1002

———————

STRESS ANALYSIS OF COLUMNS AND BEAM COLUMNS

BY THE PHOTOELASTIC METHOD

By B. F. Ruffner

SUMMARY

Principles of similarity and other factors in the design of models for photoelastic testing are discussed. Some approximate theoretical equations, useful in the analysis of results obtained from photoelastic tests, are derived. Examples of the use of photoelastic techniques and the analyses of results as applied to uniform and tapered beam columns, circular rings, and statically indeterminate frames, are given. It is concluded that this method is an effective tool for the analysis of structures in which column action is present, particularly in tapered beam columns, and in statically indeterminate structures in which the distribution of loads in the structures is influenced by bending moments due to axial loads in one or more members.

INTRODUCTION

Many authors have discussed methods for determining the bending moments and buckling loads in columns and beam columns. Niles and Newell (reference 1) give solutions of the problem for various loading conditions with the EI of the beam constant for the span under consideration. Timoshenko (reference 2, p. 128) gives the critical buckling loads for tapered columns of several types. The problems discussed in those references represent solutions of the basic differential equation of a beam loaded with an axial load P and lateral loads $q(x)$. This differential equation is:

$$EI \frac{d^2 y}{dx^2} + Py = f(x) \tag{1}$$

When EI is a constant, this equation yields readily to integration and the bending moments M_x at any section x are given by:

$$M = f(x) - Py \qquad (2)$$

The critical load P_{cr} is:

$$P_{cr} = \frac{C\pi^2 EI}{l^2} \qquad (3)$$

where C is the fixity coefficient depending on the end conditions of the beam. The value of P_{cr} is independent of the lateral loading q(x).

In many cases, however, EI is not constant but varies either continuously or discontinuously over the length of the span under consideration. Equation (1) may then be integrated by approximate numerical methods. General solutions are possible only in a few cases.

It is the purpose of this investigation to develop a simple, accurate, and quick method of determining moments and critical loads in members loaded as beam columns by the use of methods of photoelastic analysis. The method will be most useful for statically indeterminate structures containing members with nonlinear behavior.

This investigation, conducted at the Oregon State College, was sponsored by and conducted with the financial assistance of the National Advisory Committee for Aeronautics.

DESIGN OF PHOTOELASTIC MODELS

General Considerations

In order for a model test to be useful it must be possible to predict accurately results on the full-scale structure from results of the model test. To accomplish this purpose, it is necessary to design photoelastic

models with several fundamental principles in mind. First, principles of similarity must be met between the model and full-scale. Secondly, the model must be constructed so that limitations imposed by techniques of testing are considered. Thirdly, the models must be of such dimensions that they can be constructed within tolerances required.

Similarity Principles

By use of dimensional analysis it is possible to determine the conditions of similarity that must be met in structural models. (See reference 3.) If P is any one external load on a structure, $\gamma_1 P, \gamma_2 P, \gamma_3 P \ldots$, are any other external loads on the structure, $l_1, l_2, l_3, l_4 \ldots$, are pertinent linear dimensions of the structure, E is modulus of elasticity, μ is Poisson's ratio, then it may be shown that, in general,

$$\frac{R}{P} = f_1 \left(\frac{P}{E l_1^2}, \gamma_1, \gamma_2, \gamma_3 \ldots, \frac{l_2}{l_1}, \frac{l_3}{l_1}, \frac{l_4}{l_1} \ldots \mu \right) \tag{4}$$

$$\frac{M}{P l_1} = f_2 \left(\frac{P}{E l_1^2}, \gamma_1, \gamma_2, \gamma_3 \ldots, \frac{l_2}{l_1}, \frac{l_3}{l_1}, \frac{l_4}{l_1} \ldots \mu \right) \tag{5}$$

where R is any reaction or internal force in a member, and M is a bending moment in a member.

If all the parameters on the right-hand side of the equation are the same on the model and the full-scale structure, the left-hand members will be the same for the model and the full-scale structure. Values for the full-scale structure would then be obtainable from model test.

In certain particular cases it is unnecessary to have all the nondimensional parameters the same on the model and the full-scale structure, since some are not pertinent. Several types of structures will be briefly discussed.

STRUCTURES IN WHICH MOMENTS, INTERNAL LOADS, REACTIONS,
AND SO FORTH, ARE LINEAR FUNCTIONS OF THE LOADS

In many structures the forces in the members, the stresses, deformations, and so forth, are all linear functions of the load. Then the nondimensional parameter P/El_1^2 is not significant. If the ratios R/P and M/Pl_1 are determined for any one set of loads, they are then the same for any other set of loads in constant ratios to the first set.

In most structures of this type Poisson's ratio μ is not significant either. For instance, consider the problem of bending of beams in which the equation:

$$EI \frac{d^2 y}{dx^2} = M$$

is applicable. Since μ does not appear in this equation, it may be considered permissible to neglect this parameter. If the beam is loaded so that M is not a function of y, then both P/El_1^2 and μ may be neglected. Furthermore, geometrical similarity is not necessary for the determination of moments, reactions, and so forth, since the linear dimensions of the cross sections come in only as influencing the moment of inertia. Consequently, the similarity conditions to be met would be expressed by the equations:

$$\frac{R}{P} = f_1 \left(\gamma_1, \gamma_2, \gamma_3 \cdots \frac{l_2}{l_1}, \frac{l_3}{l_1} \cdots \frac{I_1}{l_1^4}, \frac{I_2}{l_2^4} \cdots \right) \quad (6)$$

$$\frac{M}{P} = f_2 \left(\gamma_1, \gamma_2, \gamma_3 \cdots \frac{l_2}{l_1}, \frac{l_3}{l_1} \cdots \frac{I_1}{l_1^4}, \frac{I_2}{l_2^4} \cdots \right) \quad (7)$$

These conditions require that the loads on the model and the full-scale structure be in the same ratio, that the lengths $l_1, l_2, l_3 \ldots$ of the neutral axes of various members of the model and the structure be in the same ratio,

and that the moments of inertia of various parts of the structure be in the same ratio on the model and the full-scale structure.

COLUMNS AND BEAM COLUMNS WITH STATICALLY DETERMINATE

EXTERNAL LOADS

Structures which behave nonlinearly, but which are loaded so that the material is in the elastic range everywhere, include those structures classed as columns and beam columns.

The basic equation of the elastic curve for these is:

$$EI \frac{d^2 y}{dx^2} = M$$

but in this case M is a function of both x and y. For instance, consider a beam column of length l with $EI = f(x)$. The equation of the elastic curve of this may be written:

$$\frac{d^2 \left(\frac{y}{l}\right)}{d\left(\frac{x}{l}\right)^2} + \frac{Pl^2}{EI}\left(\frac{y}{l}\right) = k \frac{Wl^2}{EI} f_1\left(\frac{x}{l}\right)$$

where P is the axial compressive load and $kW f_1\left(\frac{x}{l}\right)$ is the bending moment due to lateral loading W, composed of loads $\gamma_1 P$, $\gamma_2 P \ldots$, and so forth.

In order for this equation to be identical for both model and full-scale structure, the conditions that

$$\left(\frac{Pl^2}{EI}\right)_m = \left(\frac{Pl^2}{EI}\right)_s$$

and

$$\left(\frac{Wl^2}{EI}\right)_m = \left(\frac{Wl^2}{EI}\right)_s$$

must be met at every point defined by $\dfrac{x}{l}$. The subscript m

is used to denote model, and the subscript s to denote full-scale structure. Dividing the first of these equations by the second gives:

$$\left(\frac{P}{W}\right)_m = \left(\frac{P}{W}\right)_s$$

Here again Poisson's ratio μ is not pertinent. The bending moment may then be written:

$$\frac{M}{Wl_1} = f\left(\gamma_1, \gamma_2, \gamma_3 \ldots \frac{l_2}{l_1}, \frac{l_3}{l_1}, \frac{Pl_1^2}{EI}\right) \tag{8}$$

It is usually more convenient to let the moment, at some point, due to all lateral loads be M_0 and write the foregoing equation in the alternate form,

$$\frac{M_0}{M} = f\left(\gamma_1, \gamma_2, \gamma_3 \ldots \frac{l_2}{l_1}, \frac{l_3}{l_1}, \frac{Pl_1^2}{EI}\right) \tag{8a}$$

If I is a variable, this must be written:

$$\frac{M_0}{M} = f\left(\gamma_1, \gamma_2, \gamma_3 \ldots \frac{l_2}{l_1}, \frac{l_3}{l_1}, \frac{Pl_1^2}{EI_0}, \frac{I_0}{I}\right) \tag{8b}$$

where I_0 is the moment of inertia of some selected section. The conditions for similarity for a column or beam-column test are then:

    1. The ratios between loads on the model and between corresponding loads on the full-scale structure should be the same.

2. The ratios of I_0/I for corresponding points in model and full-scale structure should be the same.

3. Ratios of lengths of neutral axes on model and full-scale structure should be the same.

4. Values of M_0/M then will be the same model and full scale if the ratio Pl_1^2/EI_0 is the same model and full scale.

STATICALLY INDETERMINATE STRUCTURES IN WHICH ONE OR MORE
MEMBERS IS A COLUMN OR A BEAM COLUMN

For structures of this type all similarity conditions applicable to beam columns must be met. In addition, however, the distribution of loads may depend on the cross-sectional areas of the members as well as their moments of inertia. In structures in which it is known that deformations due to direct tensile and compressive stresses are unimportant, it will be sufficient to meet only those similarity conditions listed for beam columns. If, however, both bending deformations and deformations due to tensile and compressive stresses are important, then the condition that the areas of all members must be in the same ratio model and full scale is important. Equation (5) then may be written in the form:

$$\frac{M_0}{M} = f\left(\gamma_1, \gamma_2, \gamma_3 \ldots \frac{Pl_1^2}{EI_0}, \frac{I_0}{I}, \frac{P}{A E}, \frac{A_0}{A}, \frac{l_2}{l_1}, \frac{l_3}{l_1} \ldots\right) \quad (9)$$

A_0/A is the ratio of the area of some selected section of a structural member to the area of any other section. If structures are of the type in which shear deformations also are important, then the conditions of geometric similarity must be met in addition to the foregoing. This in most structures, however, is not the case, and the model need not be geometrically similar to full scale. Usually models with members of constant thickness may be used to represent full-scale conditions.

DESIGN OF MODELS IN WHICH ONE OR MORE MEMBERS ARE LOADED

AS BEAM COLUMNS BUT IN WHICH LOADS IN MEMBERS

ARE STATICALLY INDETERMINATE

If this structure is of the type in which deformations due to tensile and compressive forces in the members are negligible as compared to deformations due to bending, then the method of design of the model and the determination of test load conditions are the same as for the beam-column models previously discussed. If, however, deformations due to tensile and compressive loads may be important, then it is necessary to meet the additional similarity condition that areas of various members on the model must be in the same ratios as corresponding areas full scale. In addition, the ratio P/EA_o for the model and the full-scale structure must be the same. To meet these conditions, in addition to the other conditions of similarity, necessitates a variation in thickness of the model material. If a structure is composed of several members each of constant EI and constant area, the model may be constructed with little difficulty if the thickness of the photoelastic model is different for each member. The model design and loading conditions then will be determined as follows:

1. Assume some convenient over-all dimension for the model. Let this be L_{om}.

2. Next designate the moment of inertia of some full-scale member as I_{os} and the area of that member A_{os}. Choose a moment of inertia which will give a reasonable model dimension, say I_{om}, for the corresponding member on the model. The dimensions of this section of the model member then may be determined to meet the necessary similarity conditions for area. From equation (9):

$$\left(\frac{PL_o^2}{EI_o}\right)_m = \left(\frac{PL_o^2}{EI_o}\right)_s$$

and

$$\left(\frac{P}{A_o E}\right)_m = \left(\frac{P}{A_o E}\right)_s$$

Dividing the first of these by the second gives:

$$\left(\frac{A_o L_o^2}{I_o}\right)_m = \left(\frac{A_o L_o^2}{I_o}\right)_s$$

or

$$A_{om} = A_{os} \left(\frac{L_{os}}{L_{om}}\right)^2 \frac{I_{om}}{I_{os}} \tag{10}$$

If I_{om} has been chosen, then the dimensions of a rectangular section of the model may be determined. If b is the thickness of the model and h the width of the section, then,

$$A_{om} = b_o h_o$$

$$I_{om} = \frac{b_o h_o^3}{12}$$

Substituting this in equation (10) gives:

$$\left. \begin{aligned} b_o h_o &= A_{os} \left(\frac{L_{os}}{L_{om}}\right)^2 \frac{b_o h_o^3}{12 I_{os}} \\[2em] h_o &= \left(\frac{L_{om}}{L_{os}}\right) \sqrt{\frac{12 I_{os}}{A_{os}}} \end{aligned} \right\} \tag{11}$$

Then,

$$b_o = \left(\frac{L_{os}}{L_{om}}\right)^3 \left(\frac{I_{om}}{I_{os}}\right) \sqrt{\frac{A_{os}^3}{12 I_{os}}} \tag{12}$$

and the model dimensions are determined for that section.

To determine other model dimensions, say at a section denoted by the subscript 1, the conditions,

$$\left(\frac{b_1 h_1}{b_0 h_0}\right) = \left(\frac{A_1}{A_0}\right)_s$$

$$\left(\frac{b_1 h_1{}^3}{b_0 h_0{}^3}\right) = \left(\frac{I_1}{I_0}\right)_s$$

must be satisfied. These give,

$$h_1 = h_0 \sqrt{\left(\frac{I_1}{I_0}\right)_s \left(\frac{A_0}{A_1}\right)_s} \tag{11a}$$

$$b_1 = b_0 \sqrt{\left(\frac{I_0}{I_1}\right)_s \left(\frac{A_1}{A_0}\right)_s^3} \tag{12a}$$

In some cases it may be necessary to try several different values of I_{0m} before a model of convenient dimensions is obtained. For the model representing structures composed of members each of constant area and moment of inertia, the model will then have its members each of constant thickness, but the thicknesses will be different for different members.

When structures have individual members of varying moment of inertia and area, both the width and the thickness of the members of the photoelastic model should vary in accordance with equations (11a) and (12a). It is not practical, however, to construct photoelastic models in this manner. Usually, the condition that the moments of

inertia of the models must vary according to $\left(\dfrac{I}{I_o}\right)_m = \left(\dfrac{I}{I_o}\right)_s$
is the most important. Good accuracy usually may be obtained if the thickness of a member is determined so that

its average area will meet the condition $\left(\dfrac{A_{av}}{A_o}\right)_m = \left(\dfrac{A_{av}}{A_o}\right)_s$.

The correct variation in moment of inertia is then obtained by varying the width of that member.

3. When the dimensions of the model have been determined, the loads to be applied to the model then are determined from the condition that

$$\left(\frac{PL_o^2}{EI_o}\right)_m = \left(\frac{PL_o^2}{EI_o}\right)_s$$

ADDITIONAL COMMENTS ON MODEL DESIGN

1. The model should be large enough so that reasonable tolerances in the construction of the model will not cause serious errors in the values of the moment of inertia. For instance, if the model can be cut to dimension within ±0.002 inch, there will be a possible error in moment of inertia of ±6 percent if the width of the model is 0.100 inch. If buckling loads are desired, this would give an error of 6 percent in estimated buckling load.

2. Usually, better fringe patterns, less "edge effect," and better photographs will be obtained with Bakelite of 0.300-inch thickness or less. If the thickness is too small, however, too few fringes may be obtained for the allowable stress in the Bakelite. The accuracy of the tests, particularly in determining bending moments and axial loads, is improved if the model is loaded so as to produce a large number of fringes. Thicknesses of Bakelite BT 61-893 from 0.125 inch to 0.300 inch give good results.

3. In constructing models of statically indeterminate structures it is well to keep in mind that slight inaccuracies in lining up supports, fitting members together, and so forth, will cause internal loads in the structure when no external loads are acting. At times it is desirable to determine the effect of misalinement of the supports on the stresses.

This, of course, may be done by following similarity princi-
ples outlined previously in determining the correct model
misalinement.

PRELIMINARY TESTS

Purpose

The purpose of these preliminary tests was to inves-
tigate experimental procedures for determining bending
moments and critical loads in pin-ended columns and beam
columns. Models were chosen which could be analyzed by the
methods given in references 1 and 2 so that a measure of
the accuracy of the experimental results could be obtained.

Models and Tests

Models were milled from sheets of polished and annealed
Bakelite BT 61-893. Dimensions of Models 1 to 11 are given
in figures 1 and 2.

Models were loaded in the frame shown in the photograph
of figure 3. In figure 4 is shown the arrangement of the
loads on the models. The loading frame was designed so that
it was possible to vary the end load P and the lateral
load Q independently.

For each loading condition a fringe photograph under
circularly polarized light was taken of the center portion
of the beam. A monochromatic light of 5461 angstrom units
was used in all tests. Fringe photographs were numbered by
the following system: Photo No. - Model No. - Test No. -
P in lb - Q in lb. Figure 5 shows a series of fringe
photographs obtained on Model 6 with Q = 4.18 lb and P
varying from 0.0 to 30.0 lb. In table I tests run on Models
1 to 11 are listed.

Model 12, shown in figure 6, was used as a tension test
specimen for the determination of the modulus of elasticity.
This specimen was loaded up to 3000 psi. The strains were
measured by Huggenberger tensometers. The modulus of elas-
ticity was found to be 668,000 psi.

Results

Because of the symmetrical loading on the models of this preliminary series of tests, the sections at the centers of the spans of the beams are all sections of maximum moment. At these sections of maximum moment the vertical shear is zero and the only stress acting is the fiber stress

$\sigma = -\dfrac{M_c z}{I} - \dfrac{P}{A}$, where z is the distance from the neutral axis of the beam, measured in the plane of the loads, positive toward the upper edge of the beam, and M_c is the bending moment at the center of the span. Consequently, the Mohr's circle of stress for any element in this cross section is as shown in figure 7. The principal stresses on this cross section are then $\sigma_1 = -\dfrac{M_c z}{I} - \dfrac{P}{A}$ and $\sigma_2 = 0$.

Since the fringes determined photoelastically are loci of points at which the principal stress differences are a constant, the σ_1 may be determined immediately from the fringe patterns if the fringe orders are known.

The stress-optic law may be written in the form:

$$\sigma_1 - \sigma_2 = kn \tag{13}$$

where σ_1, σ_2 are principal stresses, n fringe order, k a constant depending on the wavelength of light, the properties of the material used, and the thickness of the model in the direction of propogation of the light. At

$z = \dfrac{h}{2}$ let $n = n_T$, and at $z = -\dfrac{h}{2}$, let $n = n_B$. Then,

$$\sigma_{1_T} = kn_T = \frac{-M_c h}{2I} - \frac{P}{A}$$

$$\sigma_{1_B} = kn_B = \frac{M_c h}{2I} - \frac{P}{A}$$

Solving these simultaneously for M_c gives,

$$M_c = -\frac{Ik}{h}(n_T - n_B) \tag{14}$$

If the loading of the beam is such that the bending moment is known from principles of statics, equation (14) may be used to determine k. In many tests the ratio M_{oc}/M_c is the desired variable. From equation (14) this is:

$$\frac{M_{oc}}{M_c} = \frac{(n_T - n_B)_{P=0}}{(n_T - n_B)_P} \tag{15}$$

In table I are recorded the fringe order differences $(n_B - n_T)$ for all preliminary tests run. Also in table I are given values of M_{oc}/M_c. These were obtained by dividing $(n_B - n_T)$ for the test with no axial load, by the values of $(n_B - n_T)$ obtained on each of the other tests of the same model with varying values of the axial load P. For Models 1 to 6 the theoretical critical loads are $P_{cr} = \pi^2 EI/l^2$. These were computed and entered in table I. For the tapered Models 7 to 11, the critical loads were computed by interpolating the tables given by Timoshenko in reference 2, page 128. These also are listed in table I.

In figures 8, 9, and 10 are plotted the results of tests on Models 1 to 11. Faired curves were drawn through the experimentally determined points and terminated at the computed values of P_{cr}. An inspection of these curves shows that points do not lie on the faired curves within the limits of error in the determination of moments from the photoelastic fringe patterns. The scattering of these points was believed to be due to friction in the end supports.

An examination of these curves also shows considerable variation from the straight-line plots that were expected from theoretical considerations. The curvature of these plots was believed to be due to eccentricities in the application of the end loads. To check this, the following approximate analysis of the effect of eccentricities was made.

<center>Approximate Theoretical Analysis of Effect

of Eccentricities and End Couples</center>

If eccentricities existed on Models 1 to 11, it was known that these were small. The exact amount of these

eccentricities could not be determined accurately by measurement. Therefore, the following approximate analysis was made to attempt to evaluate these eccentricities from the test results.

Timoshenko (reference 2, p. 82) has pointed out that a Fourier series may be used to represent accurately the deflection curve of a beam column. He also shows that, if only the first term of the series is used, the deflection curve, for many types of beams, is represented within required engineering accuracy. In figure 11 the notation is defined. Then, let

$$y = -a_1 \sin \frac{\pi x}{l} \qquad (16)$$

where $-a_1$ is the deflection at a point midway between the points of inflection. The bending moment M, at any point x is,

$$M = EI \frac{d^2 y}{dx^2} = \frac{\pi^2 EI}{l^2} a_1 \sin \frac{\pi x}{l} \qquad (17)$$

In general, EI may be a function of x. Let $(EI)_{eff}$ be a constant which may be substituted in (17) to give the same value of the critical load that will be obtained if the actual variation of EI is used. Equation (17) then becomes:

$$M = \frac{\pi^2 (EI)_{eff}}{l^2} a_1 \sin \frac{\pi x}{l} \qquad (17a)$$

The term $(EI)_{eff}$ will not be the average EI for the beam column. It is a value which will satisfy the equation,

$$P_{cr} = \frac{\pi^2 (EI)_{eff}}{l^2}$$

It may be considered to be the stiffness of a hypothetical uniform beam column having the same buckling load as the actual beam column under consideration.

Referring to figure 11, write the bending moment at any point x:

$$M = M_0 + \left[M_1 - P(y_1 + \delta_1) \right] \left(\frac{L - a - x}{L} \right)$$

$$+ \left[M_2 - P(y_2 + \delta_2) \right] \left(\frac{a + x}{L} \right) - Py \qquad (18)$$

Consider conditions at the point midway between the points of inflection, at $x/l = 1/2$. If the bending moment at this point is designated as M_c, and the portion of the bending moment due only to the lateral loads $q(x)$ as M_{oc}, then equating (17a) and (18) gives:

$$a_1 = \frac{M_{oc} + \left[M_1 - P(y_1 + \delta_1) \right] \left(\frac{L - a}{L} - \frac{l}{2L} \right) + \left[M_2 - P(y_2 + \delta_2) \right] \left(\frac{a}{L} + \frac{l}{2L} \right)}{\frac{\pi^2 (EI)_{eff}}{l^2} - P} \qquad (19)$$

and

$$M_c = \frac{\beta}{\beta - P} \left\{ M_{oc} + \left[M_1 - P(y_1 + \delta_1) \right] \left(\frac{L - a}{L} - \frac{l}{2L} \right) \right.$$

$$\left. + \left[M_2 - P(y_2 + \delta_2) \right] \left(\frac{a}{L} + \frac{l}{2L} \right) \right\} \qquad (20)$$

where

$$\beta = \frac{\pi^2 (EI)_{eff}}{l^2} \qquad (21)$$

For certain loading conditions, equation (20) may be greatly simplified. Consider, for instance, the following example: Beam column with pin ends, no end couples. For this case, $l = L$, and $M_1 = M_2 = \delta_1 = \delta_2 = a = b = 0$. Then equation (20) becomes:

$$M_c = \frac{\beta}{\beta - P} \left[M_{oc} - P \left(\frac{y_1 + y_2}{2} \right) \right]$$

or

$$\frac{M_{oc}}{M_c} = \frac{\beta - P}{\beta \left[1 - \frac{P(y_1 + y_2)}{2M_{oc}} \right]} = \frac{\beta - P}{\beta \left[1 - \frac{P}{\beta} e \right]} \tag{22}$$

where

$$e = \frac{\beta(y_1 + y_2)}{2M_{oc}} \tag{23}$$

Let $\alpha = P/\beta$; then equation (22) becomes,

$$\frac{M_{oc}}{M_c} = \frac{1 - \alpha}{1 - \alpha e} \tag{24}$$

Equation (24) indicates several interesting results:

1. If the eccentricities y_1 and y_2 are zero, then $e = 0$, and M_{oc}/M_c versus P should plot as a straight line.

2. The greater the value of the moment M_{oc} due to the lateral loading, the less the ratio e and the less will be the effect of any eccentricity on the results.

3. If the plot of M_{oc}/M_c versus P is not a straight line, however, the experimental curve may be analyzed to determine the amount of eccentricity present during the test.

If the average eccentricity $\frac{y_1 + y_2}{2}$ is denoted by y_{av}, equation (22) may be written in the form:

$$y_{av} = \frac{M_{oc} - M_c}{P} + \frac{M_c}{\beta} \tag{25}$$

The test results give values of M_{oc} and M_c for various loads P. Consequently, the experimental results may be substituted in equation (25) and β and y_{av} computed. For instance,

Let $M_{C_1} = 2M_{OC}$, and P_1 be the corresponding axial load

$M_{C_2} = 4M_{OC}$, and P_2 be the corresponding axial load

Substituting these in equation (25) and solving the result-ing equations simultaneously, gives:

$$\beta = \frac{2P_1 P_2}{3P_1 - P_2} \qquad (26)$$

and

$$y_{av} = -\frac{M_{OC}}{P_1} + \frac{2M_{OC}}{\beta} \qquad (27)$$

Critical loads for Models 1 to 11 were computed from equation (26). Values of P_1 and P_2 were taken from the faired curves of figures 8, 9, and 10. In table II are shown results of these computations. With the exception of tests on Models 1 and 2 the values of critical loads obtained from equation (26) are in good agreement with the theoretical values.

The calculated values of the eccentricities, obtained from equation (27), indicate that relatively small errors in model construction will account for rather large variations from straight-line plots shown in figures 8, 9, and 10. From this analysis of the results obtained in the preliminary tests, several tentative conclusions were drawn in regard to the best test procedure.

1. The factor $e = \frac{\pi^2 (EI)_{eff} \, y_{av}}{M_{OC}}$ should be as small as possible to avoid effects of eccentricities. This may be done by using rather large lateral loads which make M_{OC} large, or by keeping the eccentricity y_{av} as small as possible.

2. Since any error in M_{OC} will appear in all points,

the fringe values for the loading conditions with no axial
load should be determined to a high degree of accuracy.
Less possibility for errors will exist in the determination
of M_{oc} if the fringe order difference $(n_T - n_B)$ for this
condition is in the order of 8 to 10 fringes.

3. The model should be loaded with axial loads up to an
amount producing $M_c = 4M_{oc}$ (approximately). This will
assure a more accurate determination of values P_1 and P_2
for use in equation (26), and consequently a more accurate
determination of β.

4. At a moment $M_c = 4M_{oc}$ the stress $\sigma = -P/A - M_c h/2I$
in the model should not exceed the elastic limit of the model
material.

5. The pin-end connections should be in good bearings to
prevent the effect of the formation of a friction couple at
the pins. Pin friction will have the effect of giving an
effective increase in the fixity coefficient.

TESTS TO CHECK CONCLUSIONS BASED ON RESULTS

OF PRELIMINARY EXPERIMENTS

Beam Columns with Eccentricities

Models and Tests

Models 13, 14, 15, and 16 were constructed as shown in
figures 1, 12, 13, and 14. During tests the effect of fric-
tion in the pin ends was eliminated as much as possible by
vibrating the loading frame before taking photographs of the
fringe pattern. Results of tests are given in tables III
and IV and on figures 15, 16, and 17.

Figure 15 indicates that experimental results on Model
13 is in good agreement with the theoretical value given by
equation (22) for $e = 0$. This shows also that the choice
of the original value of M_{oc} does not affect the plot of
M_{oc}/M_o provided the values of M_{oc} are large enough to
produce sufficient fringes for accurate determination of
$n_T - n_B$.

Figures 16 and 17 show the comparison of experimental values of M_{oc}/M_c for Models 14, 15, and 16 with values computed from equation (24). Values of e on this curve were computed from measured values of y_1 and y_2. Table V gives values used for plots of solid lines on figures 16 and 17.

Table VI gives values of P_{cr} and y_{av} obtained by substitution of experimentally determined values of M_{oc}/M_o in equation (25). These may be compared to the theoretical values of $P_{cr} = \dfrac{\pi^2 EI}{l^2}$ and the measured eccentricities on the models.

Conclusions

1. For beam columns with constant EI and with pin ends, the use of equation (25) for extrapolating experimental results appear to give good accuracy.

2. Range of M_{oc}/M_c values from 1.0 to approximately 0.25 should be covered by the tests.

3. It is not necessary to have zero eccentricity of the end load. Results can be analyzed by use of equation (25) to find the eccentricity present in the test. If values of M_{oc}/M_c are then desired for other eccentricities, these may be obtained by use of equation (25) for any other arbitrary eccentricity.

4. Eccentricities will have no effect on the critical load, but may have a very large effect on the bending moments at values of axial load less than the critical load. If the bending stresses in the beam reach the yield stress at values of P less than the critical load the allowable value of the axial load P will be very greatly affected by small variations in eccentricity.

5. On the model the lateral load should be sufficient to give values of M_{oc} which are capable of accurate determination experimentally. This means that $n_T - n_B$ snould be at least 6.

TESTS OF CIRCULAR RING MODELS

Purpose

The purpose of this series of tests was to give an example of the use of the basic similarity equations, (4) and (5), and to determine whether continuous rings are structures in which the assumption of linearity of bending moment with load is applicable. The bending moment, on a ring, loaded with a diametrical load P, is usually taken as (reference 5):

$$M = PR \left(0.3183 - \frac{1}{2} \sin \theta \right) \tag{28}$$

where θ is the angle measured from a loaded diameter. At $\theta = \pm 90° = \pm \frac{\pi}{2}$, this gives:

$$\frac{M_{\pi/2}}{PR} = -0.1817$$

This formula indicates no variation of moment with variation in the ratio R^4/I or with variation in the ER^2/P ratio. However, if the deflection of the ring has any effect on the bending moment, one or both of these ratios may be significant. If the ratio ER^2/P is significant, a variation in $M_{\pi/2}/PR$ would be expected with variations in that parameter. If the moment of inertia of the ring is important, a variation in $M_{\pi/2}/PR$ with R^4/I would be expected. For the circular ring as loaded here, other ratios as specified in equation (5) are satisfied with the exception of μ, which is not significant in this problem.

Models, Tests, and Computations

Three circular ring models were constructed to dimensions shown in figure 18. These were cut from a sheet of polished and annealed Bakelite BT 61-893, 0.278 inch thick.

In table VII are listed tests run on the circular ring models. The average radius of the ring is denoted by R. Figure 19 shows a typical fringe photograph of a loaded ring.

The test covered a range of ER^2/P from 0.71×10^5 to 12.60×10^5 and a range of R^4/I from 2.99×10^4 to 22.2×10^4.

Bending moments in circular rings may be computed with fair accuracy by using the same methods as discussed for straight beams. Since, however, the bending stress is not distributed linearly in curved beams, the maximum bending moments at the point $\theta = \pm 90^\circ$ were computed, for greater accuracy, as follows:

1. The distance from the edge of the ringe to each fringe was measured on the fringe photograph. These measurements were then adjusted to model scale. Measurements were made for both $\theta = +90^\circ$ and -90°. Distances to fringes were averaged at these two stations. The fringe order was plotted versus the average distance from the edge of the model. A typical plot for Model 17 under a 25-pound load is shown in figure 20. The values are recorded in table VIII.

2. By planimeter integration of the area under the plot of n versus distance from edge of model, the average fringe order for the beam was computed. The neutral axis was then the point at which the average fringe order was equal to the fringe order of the curve of n versus distance from edge of model.

3. At various distances y from the neutral axis, the fringe orders were measured. In table IX are shown these values for Model 17 under 25-pound load. Values of y then were multiplied by fringe order n. The product ny then was plotted. Figure 21 shows the plot for Model 17, load 25 pounds. The area under the curve of ny versus y then was measured. This is designated as S.

4. The bending moment across the section under consideration may be written as,

$$M_{\pi/2} = -\int_{y_i}^{y_0} \sigma_1 y\, b\, dy \tag{29}$$

where

σ_1 normal stress on section

y distance from neutral axis

b thickness of ring

y_0 distance from neutral axis to outer edge of ring

y_i distance from neutral axis to inner edge of ring

From equation (13), since $\sigma_2 = 0, \sigma_1 = kn$, equation (29) becomes

$$M_{\pi/2} = -kb \int_{y_i}^{y_0} n\, y\, dy$$

Therefore,

$$M_{\pi/2} = -k\, b\, S \qquad (30)$$

For more detailed discussion of this method of determining bending moments, see reference 5.

Results

In table VII the values of $M_{\pi/2}/PR$ are given for all tests. An examination of these results shows that for Model 17 the results are very nearly those given by equation (28). For Models 18 and 19, however, the values of $M_{\pi/2}/PR$ are somewhat higher. In figure 22 are plotted average values of $M_{\pi/2}/PR$ versus ER^2/P for constant values of the ratio R^4/I. These curves show no significant variation with ER^2/P. The variation that is shown is within experimental limits of accuracy. The curve of $M_{\pi/2}/PR$ versus R^4/I, however,

indicates an increase in the bending moment with an increase in R^4/I. At low values of the ratio R^4/I the value of $M_{\pi/2}/PR$ checks almost exactly the value given by equation (28).

Conclusions

The photoelastic results show that the bending moments on circular rings are a function of the ratio R^4/I. It is recommended that models of bulkhead rings and other similar structures be constructed so that the ratio R^4/I is the same on the model and full-scale structure. It also would be well to test the model at the same ratio of ER^2/P on the model as for the full-scale structure if this is convenient. Even though little variation with ER^2/P was shown in tests, it may be that at other values of the ratio, or for other types of loading, this would be significant.

The photoelastic tests of these rings indicate that formulas in use for the calculation of bending moments in circular rings are in error for rings of large R^4/I ratios. Furthermore these errors lead to nonconservative values.

ANALYSIS OF STATICALLY INDETERMINATE FRAME

Purpose

In statically indeterminate structures, the loads and bending moments in various members of the structure are functions of the relative stiffnesses of the members. If all members are loaded with axial loads that are small compared to their critical buckling loads, the analysis of the structure may be accomplished analytically by several commonly used methods. In structures where one or more of the members is loaded with an axial load approaching its critical load, difficulties in the analysis occur due to the variation in the effective stiffness which takes place in the axially loaded member as it approaches its critical load.

The photoelastic method is useful in analyzing such a struc-
ture, provided the model is constructed and loaded as speci-
fied by the similarity principles previously discussed.

The information desired for the stress analysis of the
structures is as follows:

1. The total load at which buckling of the column mem-
ber occurs

2. The bending moment at every point in the structure

3. The axial loads in all members of the structure

4. The shear in the members

If this information is obtained, unit stresses in the full-
scale structure may be computed.

If it were not for the effect of variation of effective
stiffness in the column member as its load is increased, the
internal forces, reactions, bending moments, and so forth,
would be linear functions of the external loads and these
could be obtained for any convenient value of the applied
load, say P_1. The corresponding moments, internal forces,
and so forth, in the various members could then be found at
any load P_2 by multiplying observed values at any load
P_1 by the ratio of P_2/P_1.

When, however, one member of the structure is stressed
by an axial load approaching its own critical load, the dis-
tribution of the external loads among the members changes.
The stresses in the individual members are then not linear
functions of the external loads. In these structures the
load on the model must be selected so that the internal load
distribution at a desired full-scale loading condition will
be obtainable from the model results. In a structure of this
type similarity conditions as specified in equation (8b) are
applicable.

Model and Tests

To illustrate the use of the photoelastic method, two
models were constructed as shown in figure 23. These were
constructed of polished and annealed Bakelite BT 61-893.

Tests were started on Model 20, but the model failed before tests were completed. The results of these tests are not reported. Tests on Model 21 were run as follows:

1. Fringe photographs of the central portion of the vertical leg were taken with the load P on the frame varying from 40 to 100 pounds. Fringe photographs are shown in figure 24.

2. Fringe photographs of the entire frame were taken at a load P = 40 pounds. These are shown on figure 25.

3. Fringe photographs of the entire frame were taken at a load of P = 75 pounds. These are shown on figure 26.

Computations and Results

The fringe patterns of figure 24 were analyzed in a manner similar to that described for the beam-column models. Bending moments at a point 3.80 inches from the pin point in the vertical member were determined. These are given in table X. These moments correspond to the moment M_c in equation (25).

In order to analyze the results of this test, equation (20) is rewritten to conform to the particular loading condition on this model. If the pin end of the vertical member is considered to be equivalent to the right end of the span shown in figure 11, then,

$$M_{oc} = M_2 = y_1 = y_2 = \delta_2 = b = 0$$

Equation (20) then becomes,

$$M_c = \frac{\beta}{\beta - P'} \left[M_1 - P' \delta_1 \right] \left[\frac{L - a}{L} - \frac{1}{2L} \right] \tag{31}$$

where P' is the axial load in the vertical member.

Let $P' = \phi_1 P$

$$L = \left(l_2 - \frac{h_1}{2}\right)$$

$$M_1 = \phi_2 PL$$

Then, since δ_1, a, ϕ_1, and ϕ_2 may all be functions of P, equation (31) may be written,

$$M_c = \frac{\phi_1 \beta PL}{\beta - \phi_1 P}\left(\frac{\phi_2}{\phi_1} - \frac{\delta_1}{L}\right)\left(\frac{L-a}{L} - \frac{l}{2L}\right)$$

or

$$\frac{P\left(l_2 - \frac{h_1}{2}\right)}{M_c} = \frac{\frac{\beta}{\phi_1} - P}{\beta} f(P) \tag{32}$$

The function $f(P)$ is not, in general, determinable analytically. An examination of the physics of this, however, indicates that this function cannot be zero for any value of P. Consequently, if $\dfrac{P\left(l_2 - \frac{h_1}{2}\right)}{M_c}$ is plotted against P, this will be zero when $\dfrac{\beta}{\phi_1} - P$ is equal to zero. The value of P at this condition is then the value of the total load on the structure which will tend to produce an infinite bending moment in the vertical leg. This may be called the critical value of P for the vertical column. The critical value of P for a structure of this type may be interpreted as the total load on the structure at which the buckled member will carry no additional axial load even if P is further increased.

In figure 27, $\dfrac{P\left(l_2 - \frac{h_1}{2}\right)}{M_c}$ is plotted against P.
The curve through experimental points was extrapolated to

the point $\dfrac{P\left(l_2 - \dfrac{h_1}{2}\right)}{M_c}$ = 0.   This indicates that, at a

total load of 122 pounds, the vertical member is essenti-
ally buckled. Since the structure is redundant, this does
not necessarily mean that this is the ultimate load on the
structure. It indicates, however, that any additional load
will have to be carried entirely on the left support of the
horizontal member. Consequently, at loads above 122 pounds
the bending moments in the left portion of the beam will in-
crease much more rapidly than at loads less than 122 pounds.

To obtain the bending moment at every section of the
structure at given loads full-scale, the equivalent loads
are computed so that P/EL^2 for the model and the full-
scale structure are identical. For the tests of Model 21,
assume that these model loads have been determined to be
40 and 75 pounds.

The first step in the analysis was to determine the
fringe orders at various sections along the boundary of the
model. These were identified by observing the formation of
the fringes as the load was increased.   These fringes were
recorded on figures 25 and 26 and in tables XI and XII. At
sections of maximum moment, it is possible to plot fringe
order against depth of beam and to use faired values of
fringe orders at the boundary. At sections where bending
moments are not maximum, this method is not applicable.
Good results can be obtained, however, by using the esti-
mated values of fringe orders at the outer boundaries and
then determining the bending moments from equation (14).
This was done at various sections of the horizontal and
vertical members of Model 21 for loads of both 40 and 75
pounds. These bending moments are plotted also on figures
25 and 26. The shear forces in the members may be obtained
by measurement of the slopes of the moment curves.

The axial loads in the members may be obtained by
taking the average fringe order across the section. The
axial load is then given by:

$$P_{axial} = k \, n_{av} th$$

where   t   is the thickness and   h   the width of the cross
section. The accuracy of determination of n_{av} is poor

if the average fringe order is small. Usually, however, a
relatively large error in this axial load does not affect
the combined stress,

$$\sigma = \sigma_{av} \pm \frac{Mh}{2I}$$

to any great extent. If σ_{av} is large, then it may be
determined with greater accuracy since the average fringe
order will be larger.

In the model tested, the axial load in the column is
due to shear carried in the beam. At the 40-pound external
load the axial load in the column obtained by considering
the shear in the right-hand portion of the beam was found
to be approximately 18.0 pounds. At the 75-pound external
load the load carried by the column was found to be approxi-
mately 34.0 pounds. It is seen that the four desired items
of information for the full-scale structure are obtainable.

In beam-column structures, particularly when the beam-
column member is redundant, it is very difficult, by usual
methods, to determine allowable loads. In structures with
linear behavior, if a factor of safety on the ultimate unit
stress of 2.0 is desired, it is necessary merely to determine
the external load giving a unit stress equal to one-half of
the ultimate stress for the material and to consider this
the design load. In beam-column structures, however, ex-
ternal loads which produce bending stresses equal to one-
half the allowable stresses actually may be loads very near
the external load at which the structure will fail by buck-
ling. Also as axial loads in beam-column members approach
critical values, the bending moments increase much more
rapidly than the load. Hence ultimate stresses may be
reached at external loads very little greater than those
producing only one-half the ultimate stress at the most highly
stressed section of the beam column. In the case of long
columns, of course, loads just slightly less than the criti-
cal may produce stresses only a small fraction of the ulti-
mate stress. Tests of photoelastic models may be used to
indicate the stress conditions at various loads, and an accu-
rate determination of the allowable loads for the full-scale
structure may be made.

CONCLUSIONS

By intelligent application of the similarity principles given, photoelastic models may be constructed to represent many types of structures that cannot be readily analyzed by analytical methods. These include:

1. Beam columns of varying EI

2. Structures in which deformations are large enough so that their effect on stress distribution is not negligible (such as flexible circular rings)

3. Statically indeterminate structures in which internal forces, moments, and so forth, are not linear functions of the external loads

The examples given indicate that the techniques of test and methods of analysis used give accurate values of critical loads, bending moments, and so forth, for the photoelastic models. Corresponding full-scale values may be accurately obtained if similarity principles have been applied properly.

Oregon State College,
     Corvallis, Ore., June 1945.

REFERENCES

1. Niles, Alfred S., and Newell, Joseph S.: Airplane Structures. J. Wiley and Sons., Inc., 3d ed., vol. II, ch. XIV.

2. Timoshenko, S.: Theory of Elastic Stability. McGraw-Hill Book Co., Inc. 1st ed., 1936.

3. Goodier, J. N., and Thomson, W. T.: Applicability of Similarity Principles to Structural Models. NACA TN No. 933, 1944.

4. Roark, Raymond J.: Formulas for Stress and Strain. McGraw-Hill Book Co., Inc., p. 138.

5. Ruffner, Benjamin F.: Stress Analysis of Monocoque Fuselage Bulkheads by the Photoelastic Method. NACA TN No. 870, 1942.

TABLE I
Tests and Results on Models No. 1 to 11

Photo No.	Model No.	Test No.	P	Q	$n_B - n_T$	$\dfrac{M_{oc}}{M_c}$	Computed[•] P_{cr}
1-B	1	1	0	26.15	8.56	1.000	1200
2	1	1	0	52.30	15.90	1.000	1200
3	1	1	75	52.30	17.88	.890	1200
4	1	1	150	52.30	19.60	.812	1200
5	1	1	225	52.30	21.38	.744	1200
6	1	1	275	52.30	22.50	.707	1200
7	1	1	300	52.30	23.20	.685	1200
8	2	1	0	26.15	10.86	1.000	835
9	2	1	75	26.15	12.70	.855	835
10	2	1	150	26.15	14.52	.748	835
11	2	1	225	26.15	16.70	.651	835
12	2	1	200	26.15	16.10	.674	835
13	2	1	225	26.15	16.70	.651	835
14	3	1	0	20.92	11.70	1.000	530
15	3	1	75	20.92	14.58	.803	530
16	3	1	150	20.92	16.60	.785	530
17	3	1	225	20.92	19.60	.596	530
18	3	1	275	20.92	23.38	.501	530
19	3	1	300	20.92	26.50	.442	530
20	4	1	0	12.55	9.90	1.000	294
21	4	1	50	12.55	13.25	.747	294
22	4	1	100	12.55	16.34	.606	294
23	4	1	125	12.55	18.50	.535	294
24	4	1	150	12.55	21.30	.465	294
25	4	1	175	12.55	25.48	.389	294
26	5	1	0	7.32	9.30	1.000	146
27	5	1	25	7.32	11.34	.820	146
28	5	1	50	7.32	14.10	.659	146
29	5	1	75	7.32	19.02	.488	146
30	5	1	90	7.32	24.20	.384	146
31	5	1	100	7.32	29.28	.317	146
32	6	1	0	2.09	5.80	1.000	45.7
33	6	1	10	2.09	7.00	.828	45.7
34	6	1	15	2.09	8.20	.707	45.7
35	6	1	20	2.09	9.80	.592	45.7
36	6	1	25	2.09	11.30	.513	45.7
37	6	1	30	2.09	15.20	.381	45.7

[•]By interpolation of tables in reference (2).

TABLE I (Cont'd)
Tests and Results on Models No. 1 to 11

Photo No.	Model No.	Test No.	P	Q	$n_B - n_T$	$\dfrac{M_{oc}}{M_c}$	Computed[a] P_{cr}
38	6	1	0	4.18	11.30	1.000	45.7
39	6	1	10	4.18	14.28	.792	45.7
40	6	1	20	4.18	18.50	.612	45.7
41	6	1	25	4.18	25.80	.438	45.7
42	6	1	30	4.18	32.90	.343	45.7
43	7	2	0	26.15	10.24	1.000	401
44	7	2	75	26.15	12.30	.832	401
45	7	2	150	26.15	16.00	.640	401
46	7	2	225	26.15	19.59	.523	401
47	7	2	275	26.15	23.00	.445	401
48	7	2	300	26.15	25.58	.401	401
49	8	2	0	15.70	8.88	1.000	309
50	8	2	100	15.70	12.34	.720	309
51	8	2	175	15.70	16.16	.550	309
52	8	2	200	15.70	18.84	.472	309
53	8	2	225	15.70	23.56	.377	309
54	8	2	250	15.70	33.20	.268	309
55	9	2	0	12.55	9.54	1.000	216
56	9	2	50	12.55	12.68	.752	216
57	9	2	100	12.55	16.70	.570	216
58	9	2	125	12.55	20.38	.468	216
59	9	2	150	12.55	26.30	.362	216
60	9	2	175	12.55	41.00	.232	216
61	10	2	0	8.37	10.65	1.000	123
62	10	2	15	8.37	12.25	.869	123
63	10	2	25	8.37	13.05	.815	123
64	10	2	50	8.37	16.15	.659	123
65	10	2	75	8.37	22.45	.474	123
66	10	2	100	8.37	44.40	.239	123
67	11	2	0	4.18	10.50	1.000	45.7
68	11	2	10	4.18	14.00	.750	45.7
69	11	2	20	4.18	18.40	.572	45.7
70	11	2	25	4.18	24.35	.432	45.7
71	11	2	30	4.18	31.50	.333	45.7
72	11	2	35	4.18	43.25	.243	45.7

[a]By interpolation of tables in reference (2).

TABLE II
Analysis of Eccentricities and Critical Load

Model	P_1	P_2	$2P_1P_2$	$3P_1$	$3P_1-P_2$	$\beta = P_{cr}$ [•]	Q	M_{oc}	$-\dfrac{M_{oc}}{P_1}$	$\dfrac{2M_{oc}}{P_{cr}}$	y_{av} [+]	% error P_{cr}
1	475	805	765000	1425	620	1232	52.30	78.50	-0.1651	0.1102	-0.0549	2.9
2	330	563	371000	990	427	875	26.15	39.20	-.1187	.0895	-.0292	4.8
3	265	400	212000	795	395	536	20.92	31.40	-.1182	.1171	-.0011	1.2
4	134	213	57100	402	189	302	12.55	18.80	-.1402	.1245	-.0157	2.8
5	73	109	15920	219	110	145	7.32	11.00	-.1503	.1518	.0011	-.9
6	25	36.2	1810	75	38.8	46.6	2.09	3.14	-.1255	.1348	.0093	2.0
6	23	34.8	1602	69	34.2	46.8	4.18	6.27	-.2720	.2680	.0040	2.4
7	252	338	170200	756	418	407	26.15	39.20	-.1558	.1922	.0434	1.6
8	190	257	97700	570	313	312	15.70	23.60	-.1240	.1510	.0270	1.0
9	120	170	40800	360	190	214	12.55	18.82	-.1568	.1760	.0192	-.9
10	70	99.0	13380	210	111	125	8.37	12.55	-.1792	.2008	.0216	1.7
11	23.0	34.5	1585	69	34.5	45.8	4.18	6.27	-.2730	.2740	.0010	.2

[•] From Equation 26
[+] From Equation 27

TABLE III
Results of Tests on Model 13

Photo No.	Model No.	Test No.	P	Q	$n_B - n_T$	$\dfrac{M_{oc}}{M_c}$	Computed [°] P_{cr}
73	13	3	0	3.14	5.50	1.000	98.2
74	13	3	30	3.14	7.92	.695	98.2
75	13	3	50	3.14	11.10	.496	98.2
76	13	3	60	3.14	13.78	.399	98.2
77	13	3	70	3.14	18.06	.305	98.2
78	13	3	75	3.14	22.12	.249	98.2
79	13	3	0	6.28	11.00	1.000	98.2
80	13	3	30	6.28	15.75	.698	98.2
81	13	3	50	6.28	22.42	.490	98.2
82	13	3	60	6.28	29.00	.379	98.2
83	13	3	70	6.28	38.50	.286	98.2
84	13	3	75	6.28	45.50	.242	98.2
85	13	3	0	9.41	16.50	1.000	98.2
86	13	3	30	9.41	23.75	.694	98.2
87	13	3	50	9.41	33.80	.488	98.2
88	13	3	60	9.41	42.50	.388	98.2
89	13	3	70	9.41	54.10	.305	98.2

[°] $P_{cr} = \dfrac{\pi^2 EI}{l^2}$

TABLE IV
Tests and Results on Models 14, 15, 16

Photo	Model	P	Q	$n_B - n_T$	$\dfrac{M_{oc}}{M_c}$	$\alpha = \dfrac{P}{P_{cr\ calc}}$
			$y_{av} = -0.100''$, $e = -3.21$			
90	14	0	15.69	9.29	1.000	0
91	14	125	15.69	16.95	.548	.167
92	14	225	15.69	26.00	.357	.301
93	14	325	15.69	38.95	.239	.435
			$y_{av} = 0.100''$, $e = 3.21$			
94	14	0	15.69	8.40	1.000	0
95	14	125	15.69	5.40	1.556	.167
96	14	225	15.69	1.70	4.941	.301
97	14	450	15.69	-15.20	- .553	.602
			$y_{av} = -0.046''$, $e = -1.29$			
98	15	0	10.46	8.85	1.000	0
99	15	100	10.46	14.55	.608	.225
100	15	175	10.46	21.70	.408	.394
101	15	275	10.46	38.80	.228	.618
			$y_{av} = 0.046''$, $e = 1.29$			
102	15	0	10.46	8.57	1.000	0
103	15	100	10.46	7.78	1.102	.225
104	15	200	10.46	7.46	1.148	.451
105	15	300	10.46	5.95	1.440	.675
			$y_{av} = -0.005''$, $e = -0.11$			
106	16	0	7.32	8.97	1.000	0
107	16	60	7.32	12.04	.745	.251
108	16	100	7.32	15.42	.582	.418
109	16	160	7.32	27.53	..326	.669
			$y_{av} = 0.005''$, $e = 0.11$			
110	16	0	7.32	9.28	1.000	0
111	16	75	7.32	14.05	.660	.313
112	16	125	7.32	18.92	.490	.522
113	16	175	7.32	32.08	.289	.732

$$^{\circ}P_{cr}calc = \frac{\pi^2 EI}{\ell^2}$$

$$\text{Values from;}\quad \frac{M_{oc}}{M_c} = \frac{1 - \alpha}{1 - \alpha e}$$

α	M_{oc}/M_c $e = -3.21$	M_{oc}/M_c $e = 3.21$	M_{oc}/M_c $e = -1.29$	M_{oc}/M_c $e = 1.29$	M_{oc}/M_c $e = -0.11$	M_{oc}/M_c $e = 0.11$
.00	1.000	1.00	1.000	1.000	1.000	1.000
.05	.820	1.13	.892	1.015	.945	.955
.10	.682	1.32	.797	1.032	.889	.910
.15	.575	1.63	.712	1.053	.836	.864
.20	.488	2.22	.637	1.078	.782	.818
.25	.416	3.75	.565	1.123	.730	.772
.30	.357	17.50	.505	1.142	.678	.724
.35	.307	- 5.41	.447	1.185	.627	.675
.40	.263	- 2.14	.396	1.241	.574	.628
.45	.225	- 1.25	.347	1.312	.523	.578
.50	.192	- .83	.304	1.408	.473	.529
.55	.163	- ..59	.263	1.543	.423	.479
.60	.137	- .43	.225	1.771	.375	.428
.65	.114	- .32	.191	2.160	.326	.377
.70	.093	- .24	.157	3.090	.279	.325
.75	.073	- .18	.127	7.590	.231	.273
.80	.056	- .13	.098	-6.140	.183	.219
.85	.040	- .09	.072	-1.550	.137	.165
.90	.026	- .05	.046	- .620	.091	.111
.95	.016	- .02	.023	- .220	.045	.056
1.00	.000	.00	.000	.000	.000	.000

TABLE VI
Values of P_{cr} and y_{av} Obtained from Tests
on Models 14, 15, and 16

Model No.	Measured Eccentricity y_{av} inches	Experimental M_{oc}/M_c	Load P lb	[o]P_{cr} lb	[o]y_{av} in.	P_{cr} Theoretical
14	- 0.100	0.357	225	770	- 0.102	748
14	- 0.100	.239	325			
14	0.100	4.941	225	745	0.090	748
14	0.100	- .553	450			
15	- 0.046	0.408	175	480	0.050	445
15	- 0.046	.228	275			
15	0.046	1.148	200	468	0.040	445
15	0.046	1.440	300			
16	- 0.005	0.582	100	236	0.001	239
16	- 0.005	.326	160			
16	0.005	0.490	125	247	- 0.001	239
16	0.005	.289	175			

[o]Obtained by substitution of load P and experimental M_{oc}/M_c in Equation 25.

TABLE VII
Circular Ring Tests

Photo No.	Model No.	Test No.	Load	R	PR	$M_{\pi/2}$	$\dfrac{M_{\pi/2}}{PR}$	$\dfrac{ER^2}{P}$	$\dfrac{R^4}{I}$
114	17	7	12.5	2.30	28.8	− 5.24	−0.182	2.82×10^5	2.99×10^4
115	17	7	25.0	2.30	57.5	−10.62	− .184	1.41×10^5	2.99×10^4
116	17	7	37.5	2.30	86.3	−15.79	− .183	$.94 \times 10^5$	2.99×10^4
117	17	7	50.0	2.30	115.0	−20.58	− .180	$.71 \times 10^5$	2.99×10^4
118	18	7	5.0	2.35	11.8	− 2.33	− .198	7.36×10^5	7.93×10^4
119	18	7	10.0	2.35	23.5	− 4.35	− .185	3.68×10^5	7.93×10^4
120	18	7	13.0	2.35	30.6	− 5.86	− .192	2.84×10^5	7.93×10^4
121	18	7	16.0	2.35	37.6	− 7.21	− .192	2.30×10^5	7.93×10^4
122	18	7	18.0	2.35	42.3	− 7.90	− .187	2.05×10^5	7.93×10^4
123	18	7	20.0	2.35	47.0	− 8.84	− .188	1.84×10^5	7.93×10^4
124	18	7	23.0	2.35	54.0	−10.10	− .187	1.60×10^5	7.93×10^4
125	18	7	25.0	2.35	58.7	−10.91	− .186	1.47×10^5	7.93×10^4
126	19	7	3.0	2.38	7.15	− 1.485	− .208	12.60×10^5	22.20×10^4
127	19	7	6.0	2.38	14.30	− 2.880	− .202	6.30×10^5	22.20×10^4
128	19	7	9.0	2.38	21.40	− 4.350	− .203	4.20×10^5	22.20×10^4
129	19	7	10.5	2.38	25.00	− 4.974	− .199	3.60×10^5	22.20×10^4
130	19	7	12.0	2.38	28.55	− 5.700	− .200	3.15×10^5	22.20×10^4

TABLE VIII
Fringe Measurements for Model 17, P = 25.0 lb

Fringe order n	Distance from outer edge of photograph in inches			Distance from outer edge of model. (Model scale). inches
	$\theta = -90°$	$\theta = 90°$	Average	
4	0.035	0.025	0.030	0.041
3	.053	.055	.054	.073
2	.078	.083	.080	.108
1	.104	.107	.105	.142
0	.127	.132	.129	.174
− 1	.149	.155	.152	.205
− 2	.170	.175	.173	.232
− 3	.193	.197	.195	.263
− 4	.213	.216	.214	.289
− 5	.231	.234	.232	.313
− 6	.248	.253	.250	.338
Inner Edge	.259	.259	.259	.350

TABLE IX

Calculations for Model 17, Load = 25.0 lb

(Values of y and n from Figure 20)

Distance from neutral axis y	Fringe Order n	ny
0.183	5.41	0.990
.143	4.30	.615
.103	3.16	.326
.063	2.08	.131
.023	.75	.017
.000	.00	.000
- .037	- 1.25	.046
- .077	- 2.70	.208
- .117	- 4.15	.485
- .157	- 5.78	.908
- .167	- 6.20	1.035

TABLE X

Bending Moments in Section 3.80 in. from Pin Joint
in Vertical Member of Model 21

Photo No.	Model No.	Test No.	Load P	M_c	$\dfrac{P(\ell_2 - \frac{h_1}{2})}{M_c}$ [a]
151	21	8	40	0.875	347
152	21	8	50	1.305	291
153	21	8	60	1.750	260
154	21	8	65	2.136	231
155	21	8	70	2.410	220
156	21	8	75	2.940	194
157	21	8	80	3.580	170
158	21	8	85	4.240	152
159	21	8	90	5.440	126
160	21	8	95	6.660	108
161	21	8	100	8.200	93

[a] P, ℓ_2, h_1 defined in Figure 23.

TABLE XI
Bending Moments on Model 21, P = 40.0 lb

Horizontal Beam			
Section	Distance from left support	$n_T - n_B$	Bending moment
a	0.00	----	----
b	.30	11.2	- 20.80
c	.62	7.5	- 13.95
d	.93	3.5	- 6.50
e	1.26	0.0	0.00
f	1.56	- 3.1	5.76
g	1.87	- 7.0	13.00
h	2.20	- 10.4	19.30
i	2.50	- 13.6	25.30
j	2.82	- 16.9	31.40
k	3.13	- 20.0	37.20
ℓ	3.46	- 16.0	29.80
m	3.75	- 13.0	24.20
n	4.07	- 9.9	18.40
o	4.38	- 6.6	12.30
p	4.69	- 3.6	6.70
q_H	5.28	----	----

Vertical Column			
Section	Distance from pin joint	$n_T - n_B$	Bending moment
q_V	7.87	----	----
r	6.55	0.2	- 0.069
s	5.91	1.1	- .377
t	5.30	2.0	- .685
u	4.65	2.2	- .755
v	4.05	1.9	- .651
w	3.41	1.6	- .549
x	2.79	1.3	- .446
y	2.15	1.0	- .343
z	1.54	.9	- ..308
aa	.90	.6	- .206
bb	.28	----	----

TABLE XII
Bending Moment on Model 21, P = 75.0 lb

Horizontal Beam			
Section	Distance from left support	$n_T - n_B$	Bending moment
a	0.00	-----	-----
b	.31	23.2	- 43.20
c	.63	16.0	- 29.80
d	.93	8.5	- 15.80
e	1.26	1.0	- 1.86
f	1.56	- 5.2	9.63
g	1.88	- 12.5	23.20
h	2.19	- 19.0	35.40
i	2.51	- 25.3	47.00
j	2.82	- 33.7	62.60
k	3.14	-----	-----
l	3.44	- 33.3	61.90
m	3.75	- 27.7	51.50
n	4.06	- 22.1	41.20
o	4.38	- 15.9	29.60
p	4.70	- 10.0	18.60
q_H	5.28	-----	-----

Vertical Column			
Section	Distance from pin joint	$n_T - n_B$	Bending moment
q_V	7.86	-----	-----
r	6.55	1.4	- 0.48
s	5.94	3.5	- 1.20
t	5.31	5.9	- 2.02
u	4.68	7.4	- 2.54
v	4.05	8.2	- 2.81
w	3.43	8.3	- 2.84
x	2.80	8.0	- 2.74
y	2.18	5.4	- 1.85
z	1.55	4.3	- 1.47
aa	.92	2.3	- .80
bb	.29	-----	-----
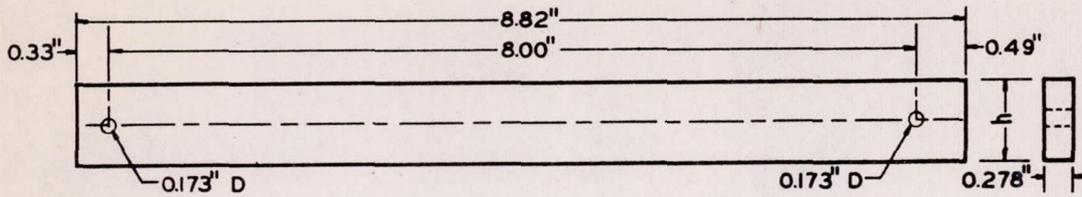
MODEL NO.	h
1	0.796"
2	0.705
3	0.605
4	0.498
5	0.396
6	0.268
13	0.346

BAKELITE BT 61-893
USED FOR ALL MODELS

Figure 1.- Dimensions of models 1, 2, 3, 4, 5, 6 and 13.
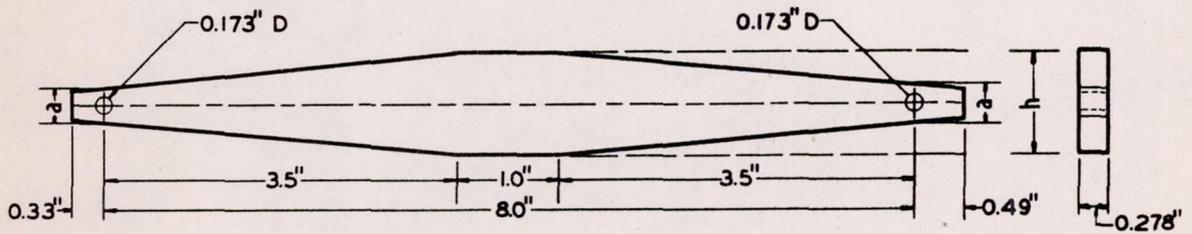
MODEL NO.	h	a
7	0.706"	0.290"
8	0.618	0.285
9	0.506	0.280
10	0.403	0.280
11	0.268	0.268

BAKELITE BT 61-893
USED FOR ALL MODELS

Figure 2.- Dimensions of models 7, 8, 9, 10 and 11.
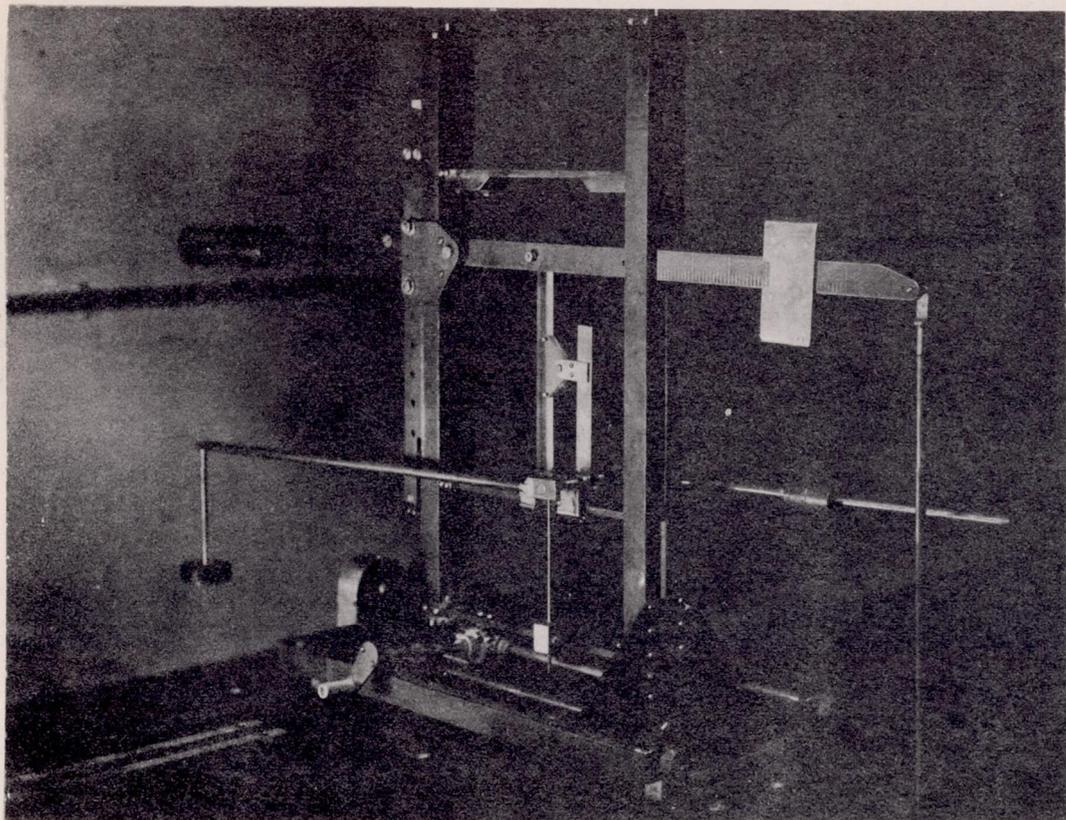
Figure 3.- Photograph of model 3 set up for test.

38-6-1-0-4.18

39-6-1-10-4.18

40-6-1-20-4.18

41-6-1-25-4.18

42-6-1-30-4.18
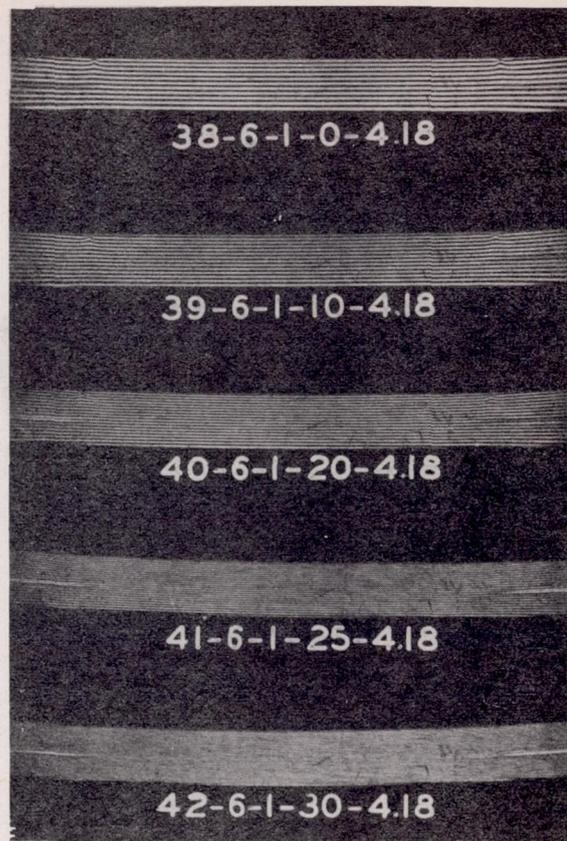
Figure 5.- Fringe photographs for model 6; P = 0 to 30 lb, Q = 4.18 lb.

Figure 4.- Positions of load applications, models 1 to 11, 13 to 16.
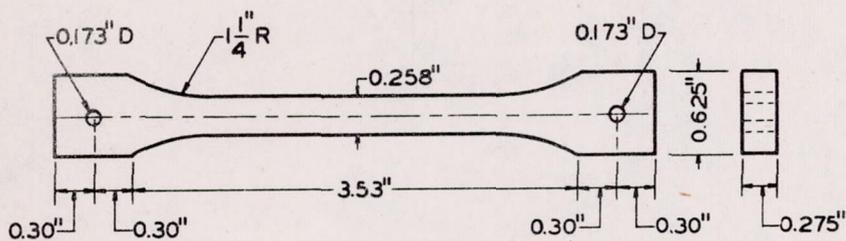
Figure 6.- Dimensions of tension test specimen, model 12.
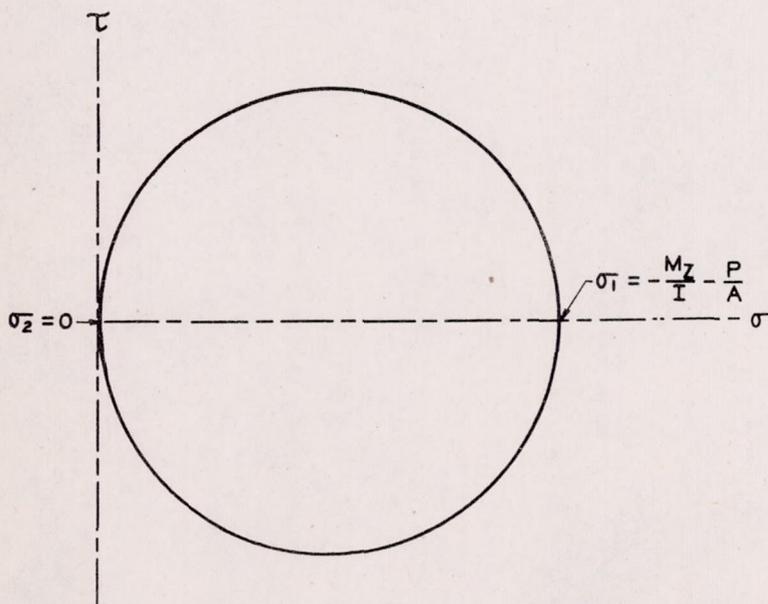
Figure 7.- Mohr's circle of stress at section of maximum moment in beam-column.
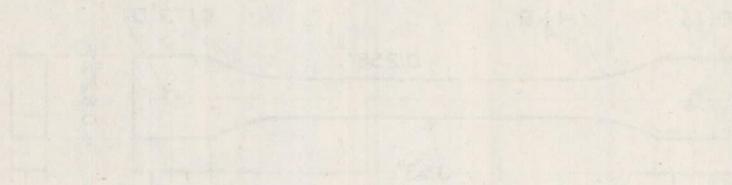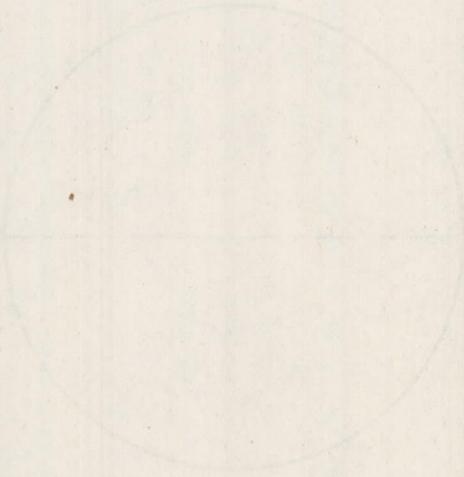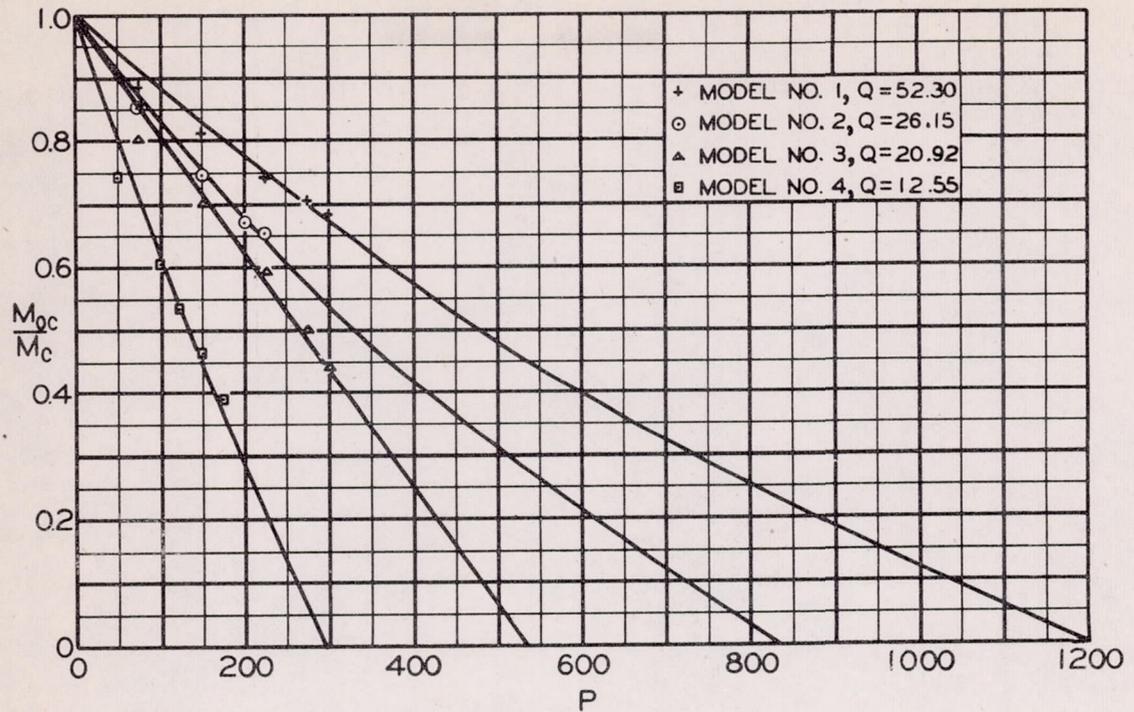
Figure 8.- Plots of M_{oc}/M_c against P for models 1, 2, 3 and 4.
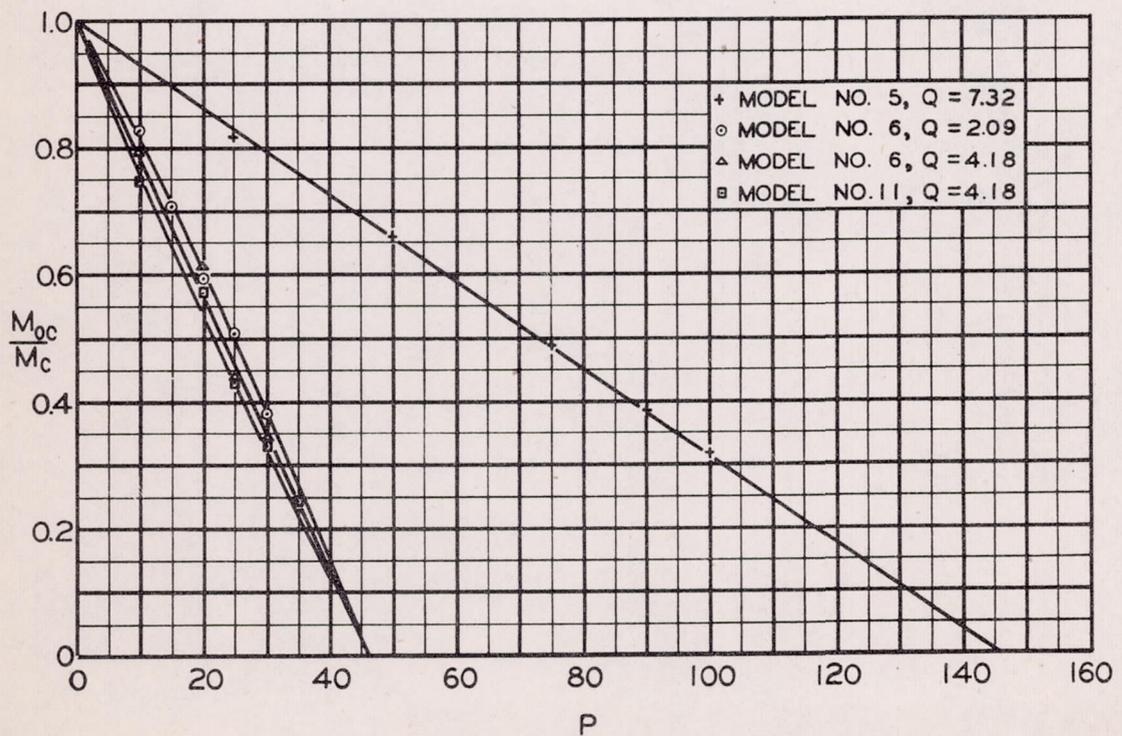
Figure 9.- Plots of M_{oc}/M_c against P for models 5, 6 and 11.
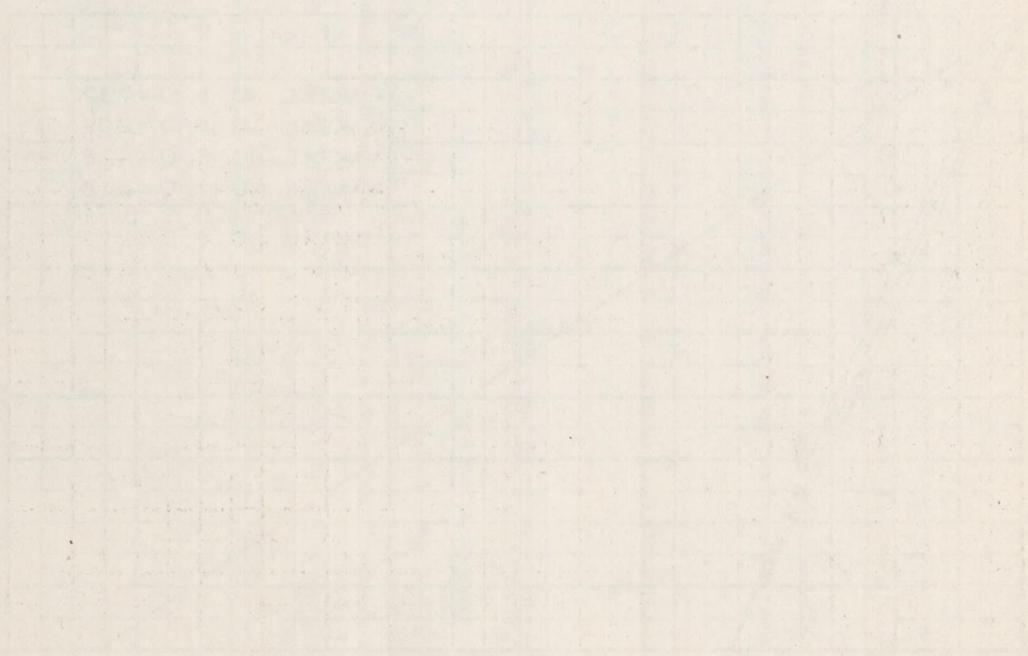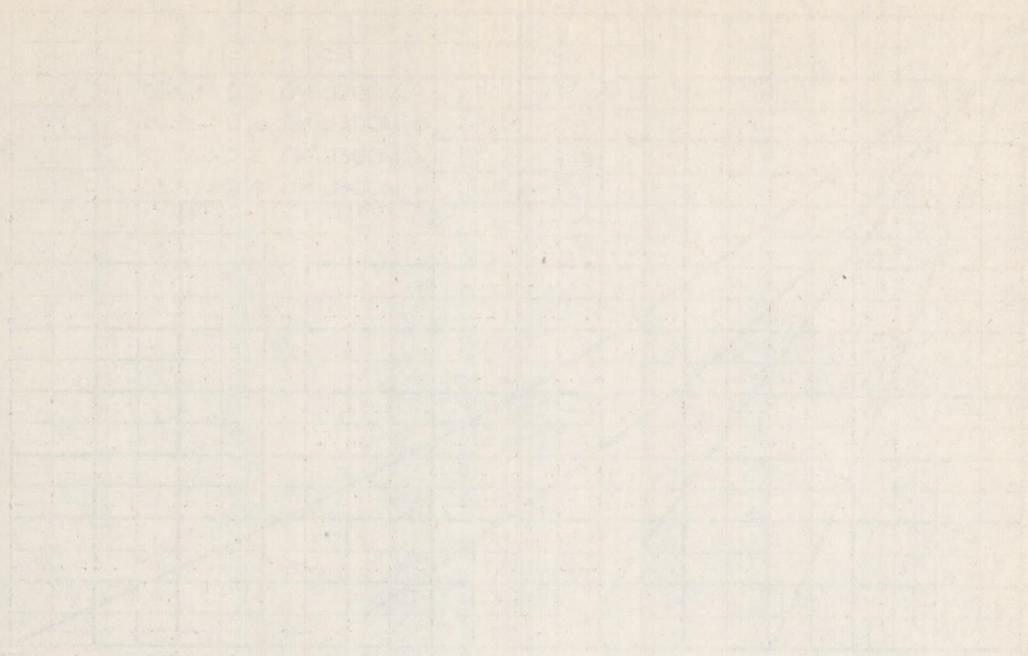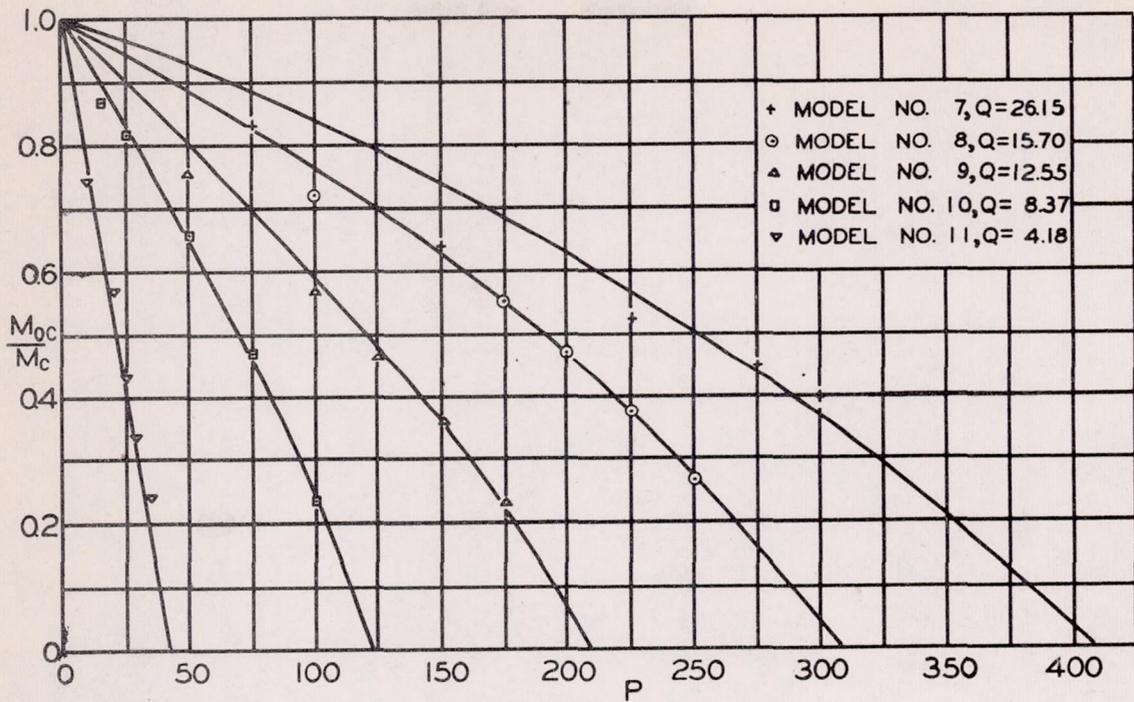
Figure 10.- Plot M_{oc}/M_c against P for models 7, 8, 9, 10 and 11.

LOAD DIAGRAM

BENDING MOMENT DIAGRAM
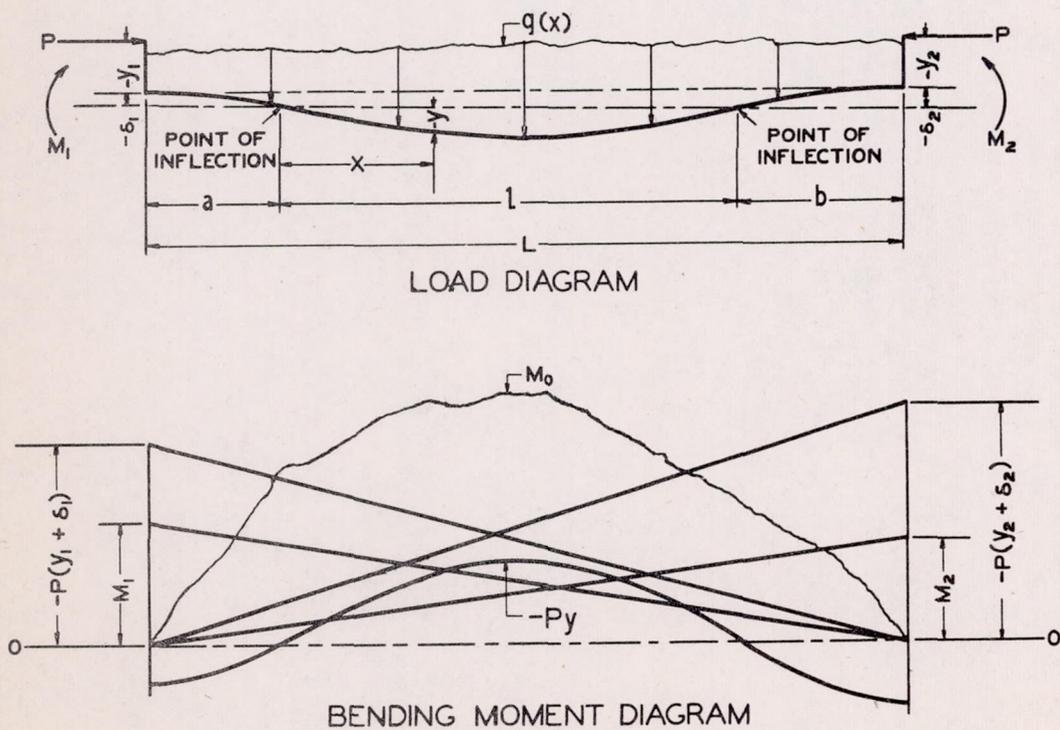
Figure 11.- Notation for beam-column span.

MODEL 14
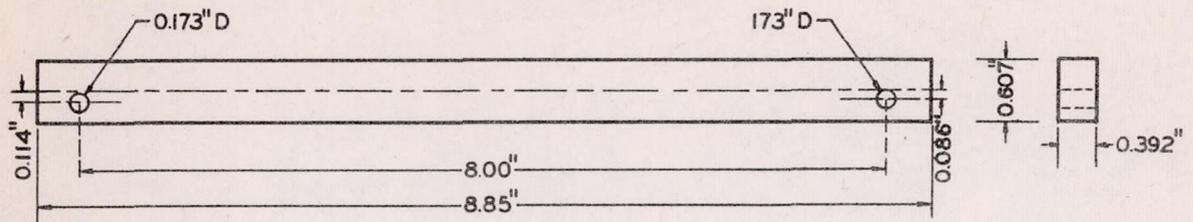
BAKELITE BT 61-893

Figure 12.- Dimensions of model 14.

MODEL 15
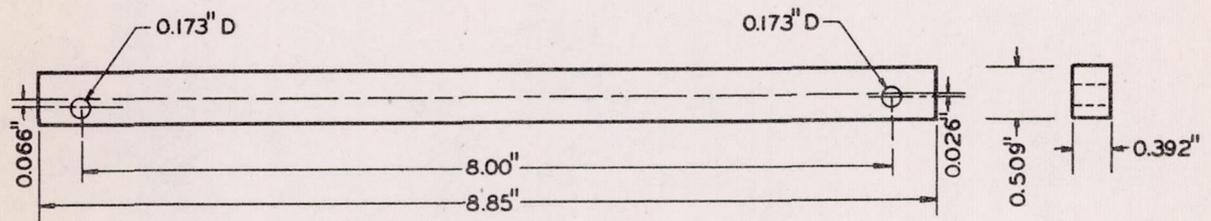
BAKELITE BT 61-893

Figure 13.- Dimensions of model 15.

MODEL 16
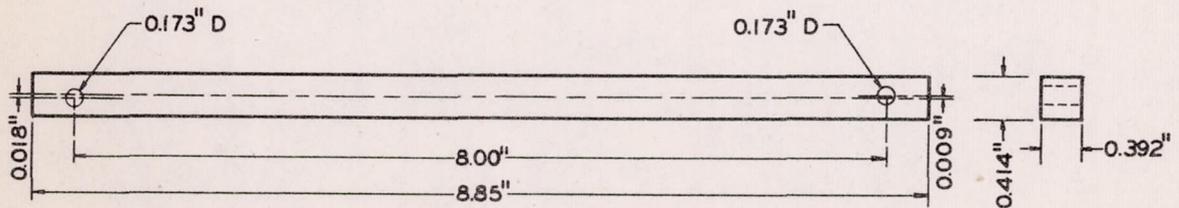
BAKELITE BT 61-893

Figure 14.- Dimensions of model 16.
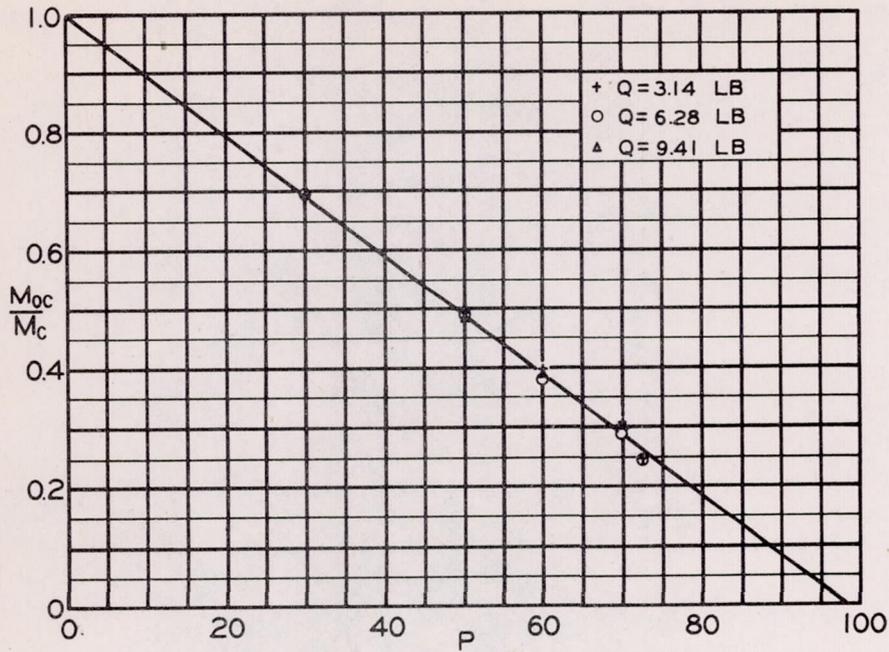
Figure 15.- Plot of M_{oc}/M_c against P for model 13.
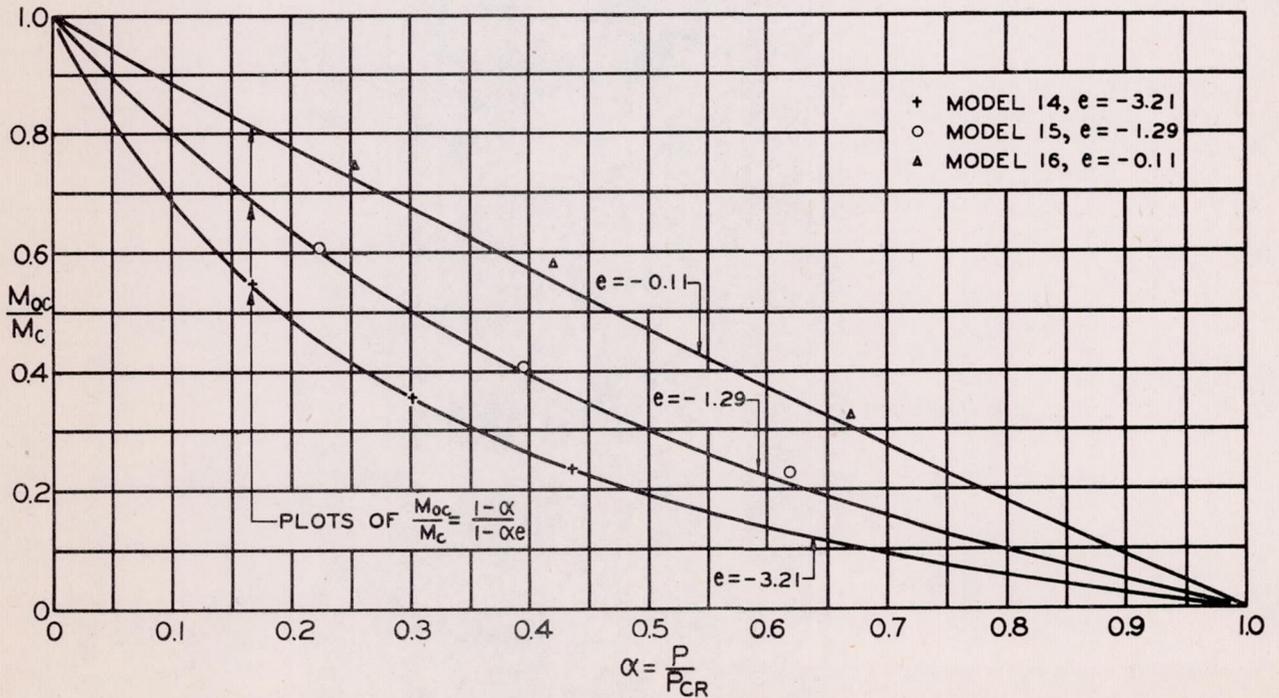
Figure 16.- Plots of M_{oc}/M_c against α for models 14, 15 and 16 with negative eccentricities.
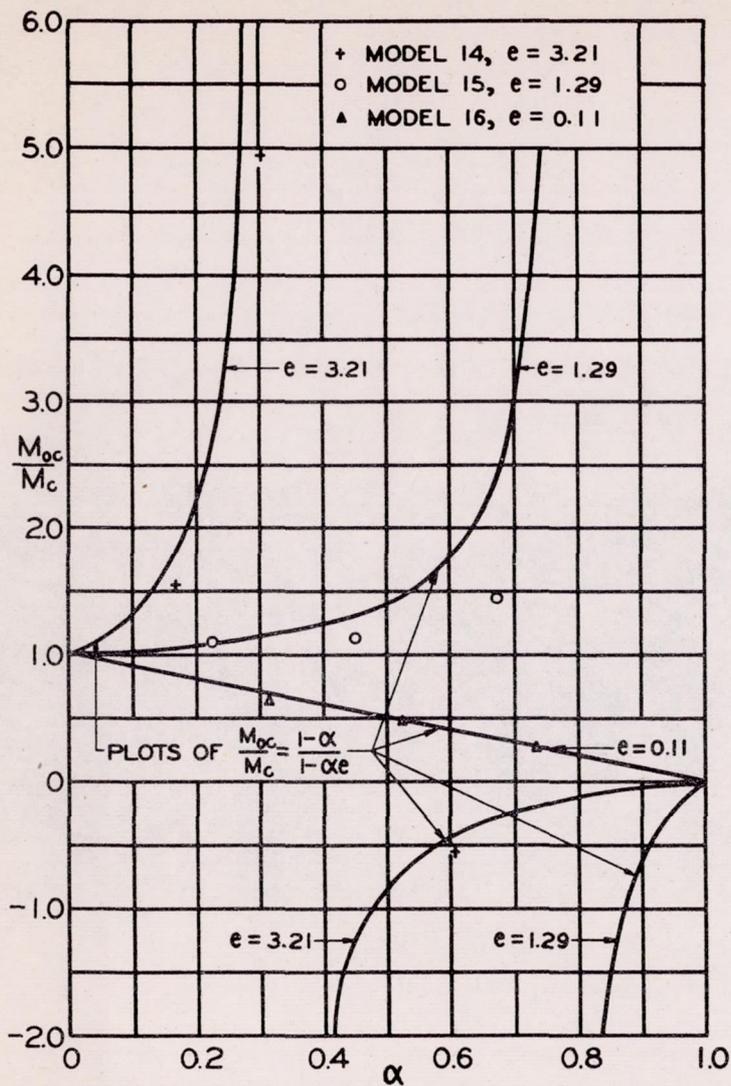
Figure 17.- Plots of M_{oc}/M_c against α for models 14, 15 and 16 with positive eccentricities.
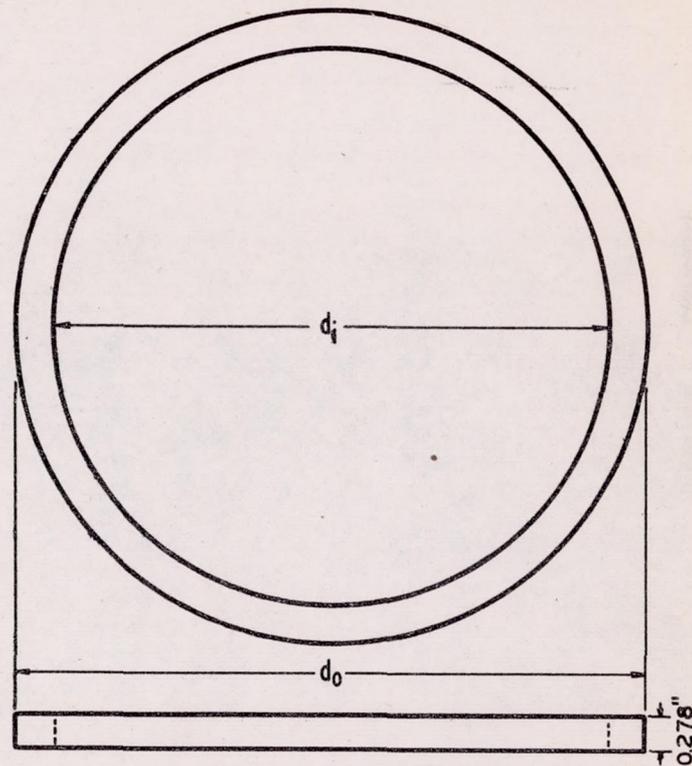
MODEL NO.	d_0	d_i
17	4.95	4.25
18	4.95	4.44
19	4.95	4.58

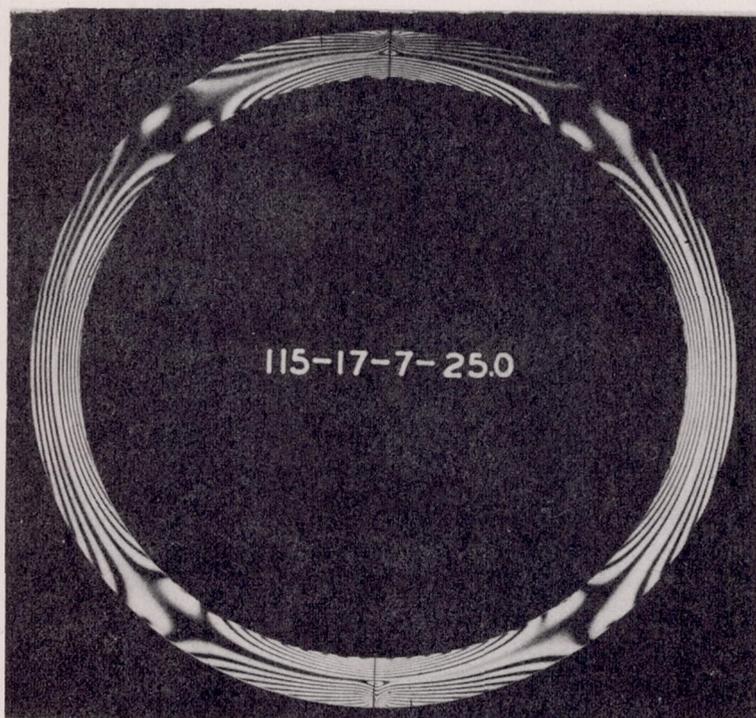Figure 18.- Dimensions of circular ring models 17, 18 and 19.

Figure 19.- Fringe photograph for model 17; P = 25 lb.
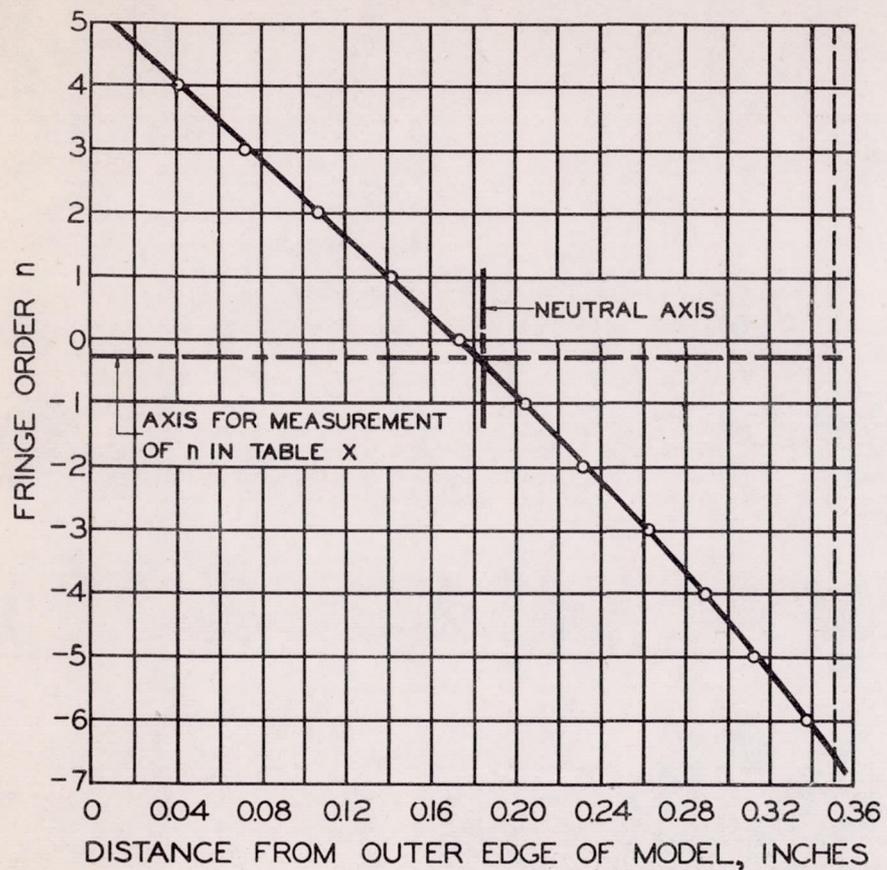
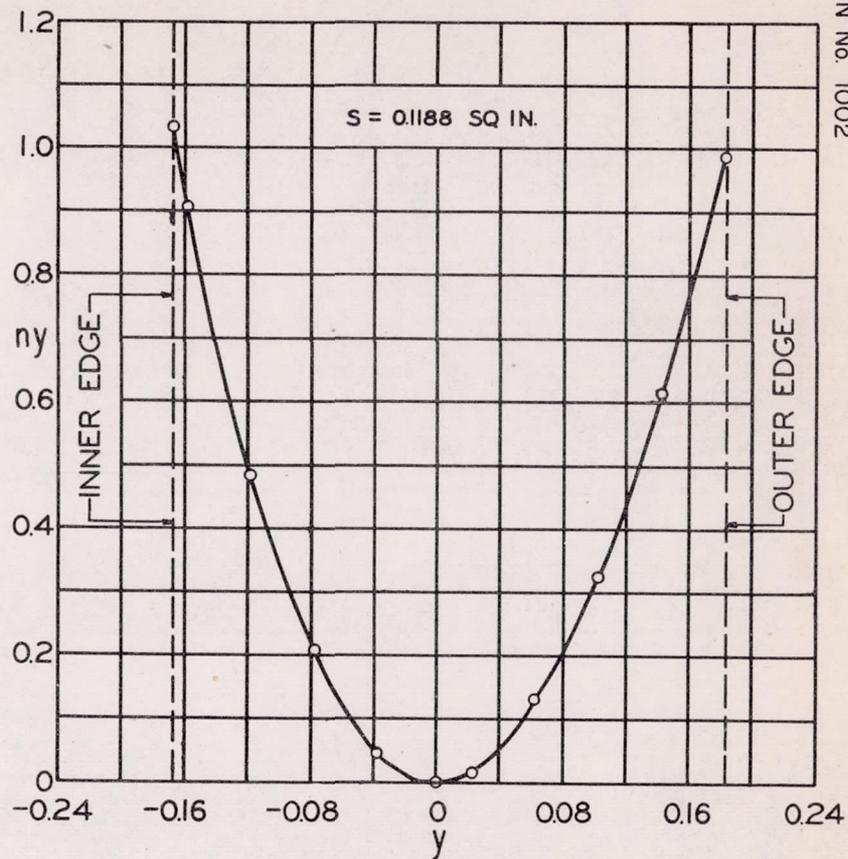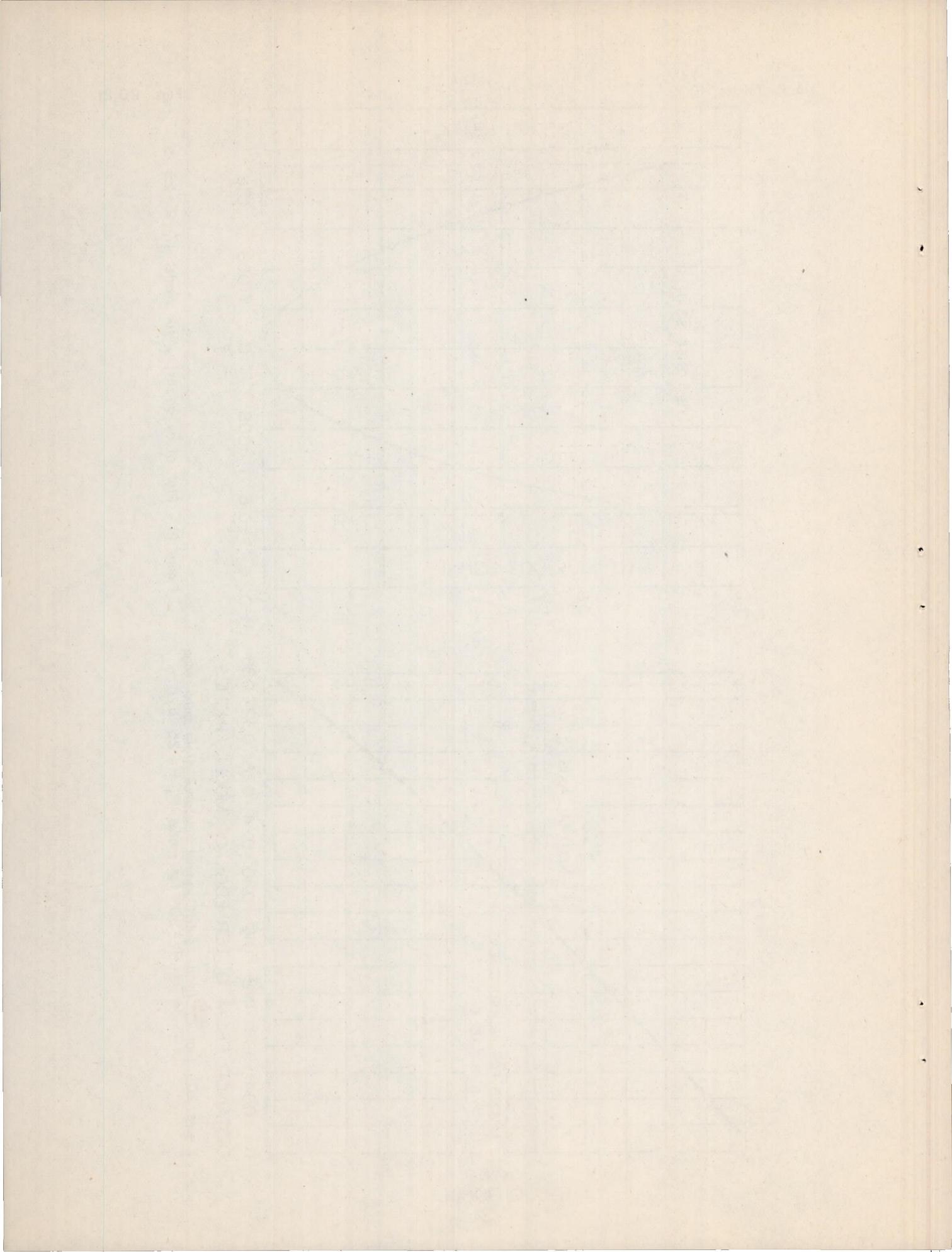Figure 20.- Plot of fringe order against distance from outer edge of model at $\theta = \pm 90°$ for model 17, P = 25 lb.

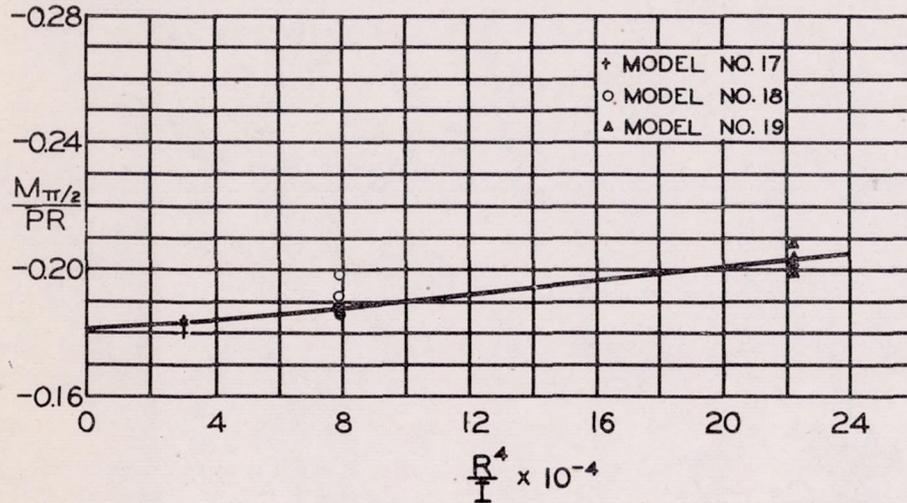Figure 21.- Plot of ny against y for model 17, P = 25 lb.
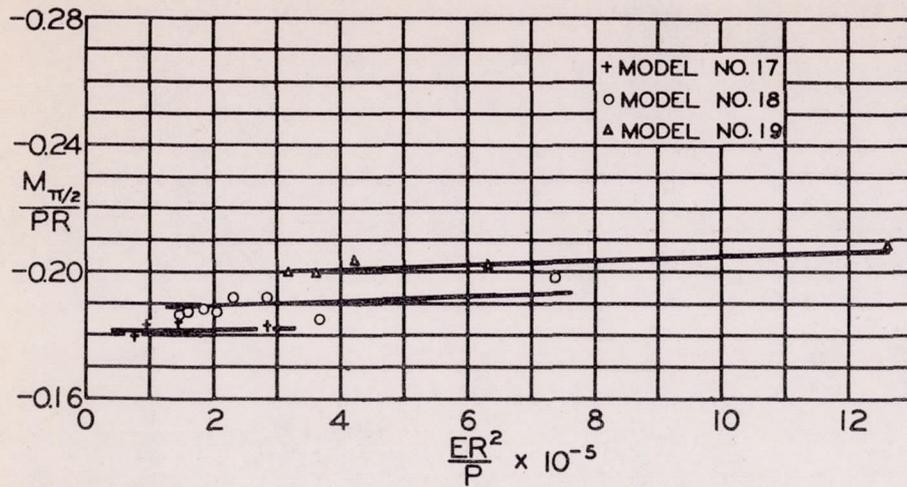
Figure 22.- Plots of $M_{\pi/2}/PR$ for circular ring models against ER^2/P and R^4/I.

t = THICKNESS
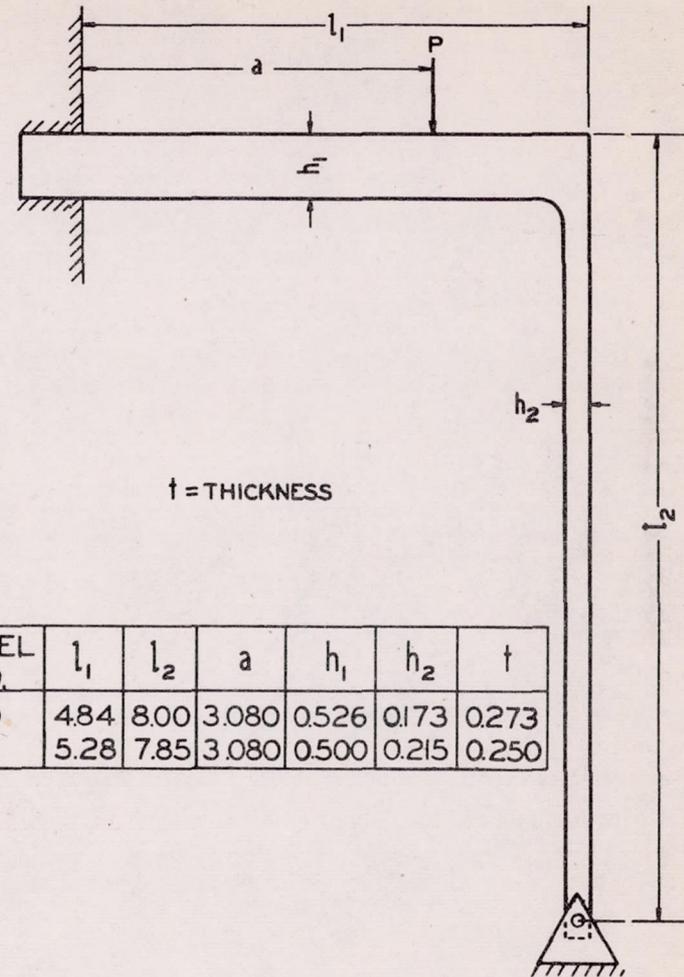
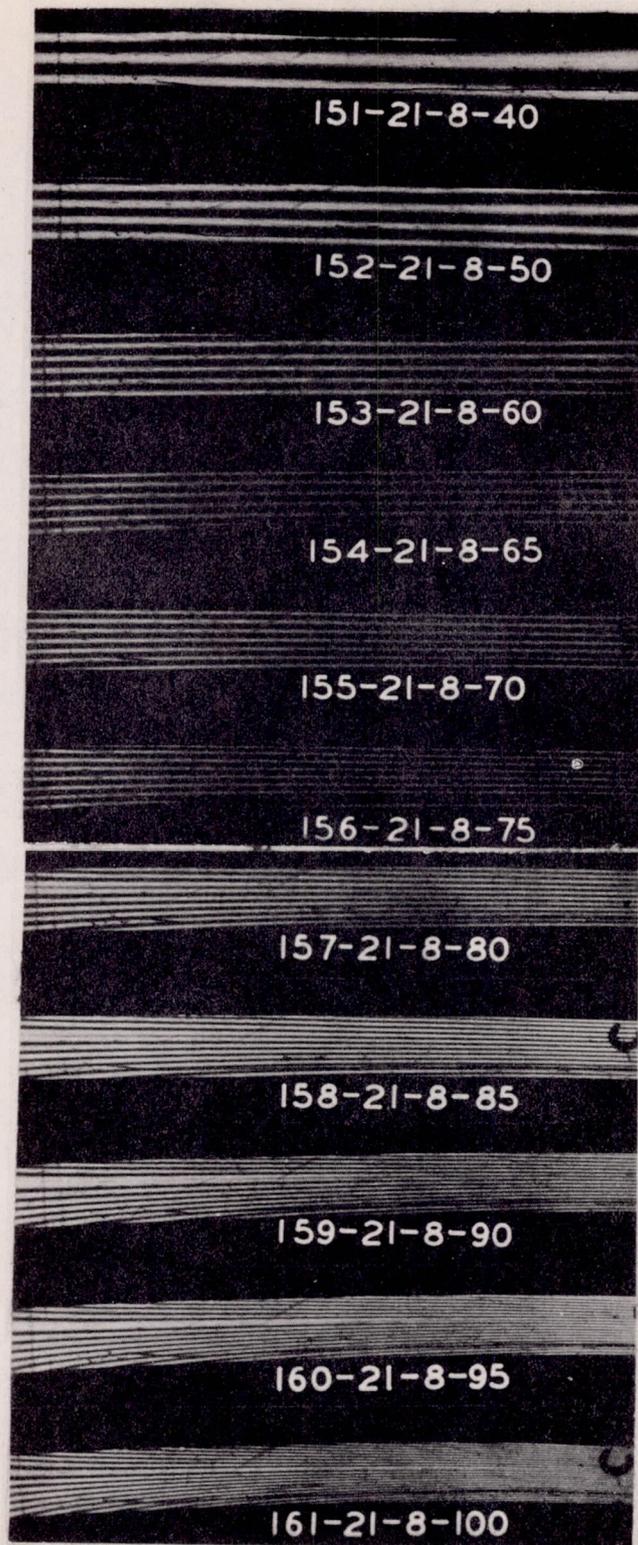| MODEL NO.	l_1	l_2	a	h_1	h_2	t
20	4.84	8.00	3.080	0.526	0.173	0.273
21	5.28	7.85	3.080	0.500	0.215	0.250

Figure 23.- Dimensions of models 20 and 21.
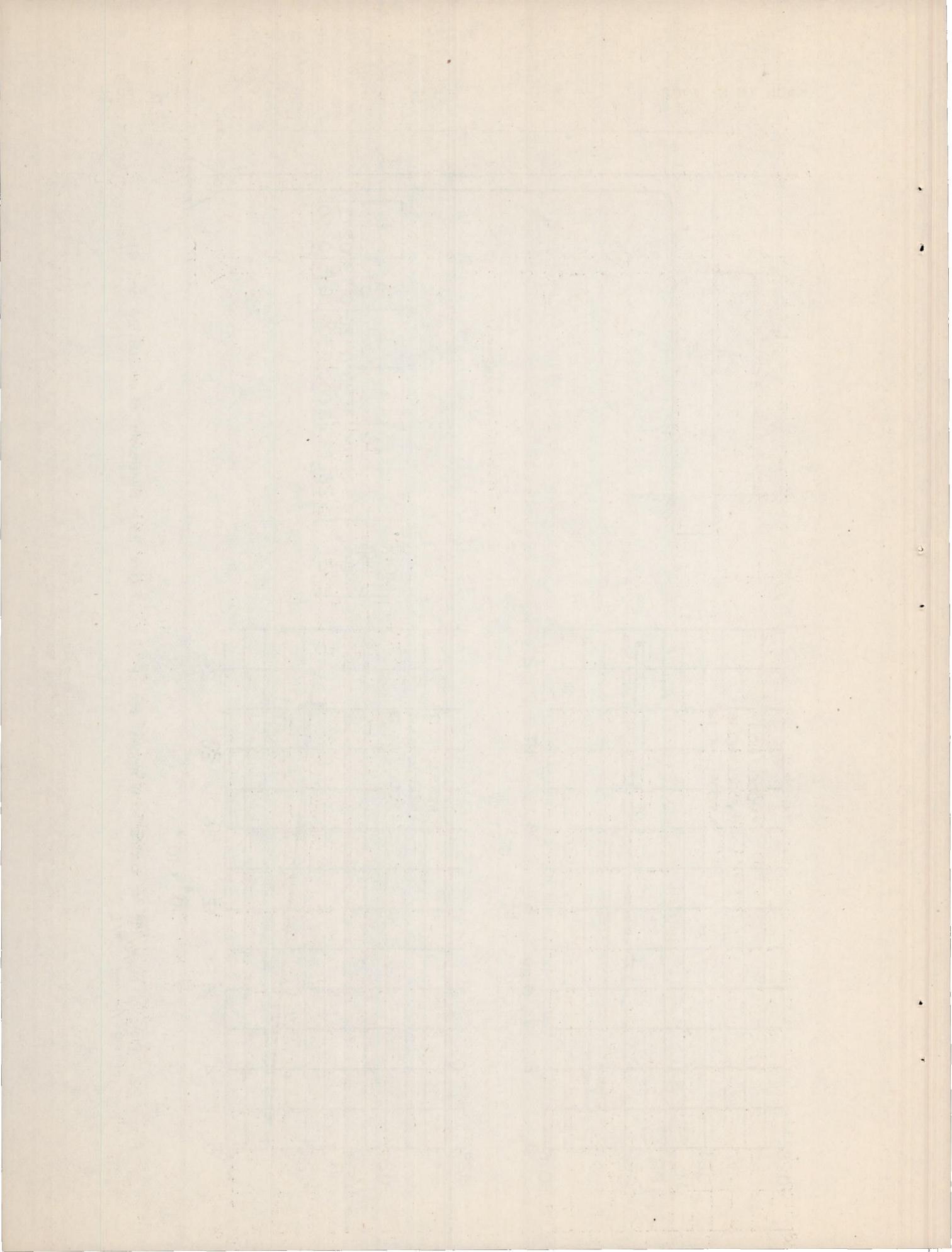
Figure 24.- Fringe photographs of mid-section of
vertical member of model 21.

Fig. 25

a

b 6.2
c 4.5
d 2.5
e 0.5
f −1.0
g −3.0
h −4.8
i −6.3
j −7.9
P = 40.0 LB
l −7.5
m −6.1
n −4.4
o −2.5
p −1.0

q_H

q_V

−5.0
−3.0
−1.0
0.5
2.1
4.0
5.6
7.3
9.0
8.5
7.0
5.5
4.1
2.6

−1.1 — −0.9 r

−1.4 — −0.3 s

−1.8 — 0.2 t

−1.9 — 0.3 u

−1.8 — 0.1 v

−1.6 — 0.0 w

−1.2 — −0.1 x

−0.9 — 0.1 y

−0.9 — 0.0 z

−0.8 — 0.2 aa

— bb

M = 37.8 IN-LB

M = 0.45 IN-LB

M = 0.45 IN-LB

MOMENT DIAGRAM

M = −26.8 IN-LB

M = −0.72 IN-LB

BENDING MOMENTS POSITIVE IF UPPER EDGE
OF BEAM OR RIGHT EDGE OF COLUMN IS IN
COMPRESSION.

NUMBERS AT SIDES OF FRINGE PHOTOGRAPHS
GIVE FRINGE ORDERS AT SECTIONS MARKED.
FRINGE ORDERS ARE POSITIVE FOR TENSILE
STRESS AT BOUNDARY.

MOMENTS IN BEAM, $M_X = -1.86(n_T - n_B)$
MOMENTS IN COLUMN, $M_y = -0.343(n_T - n_B)$.
WHERE:
n_T = FRINGE ORDER AT TOP OF BEAM AND
RIGHT SIDE OF COLUMN.
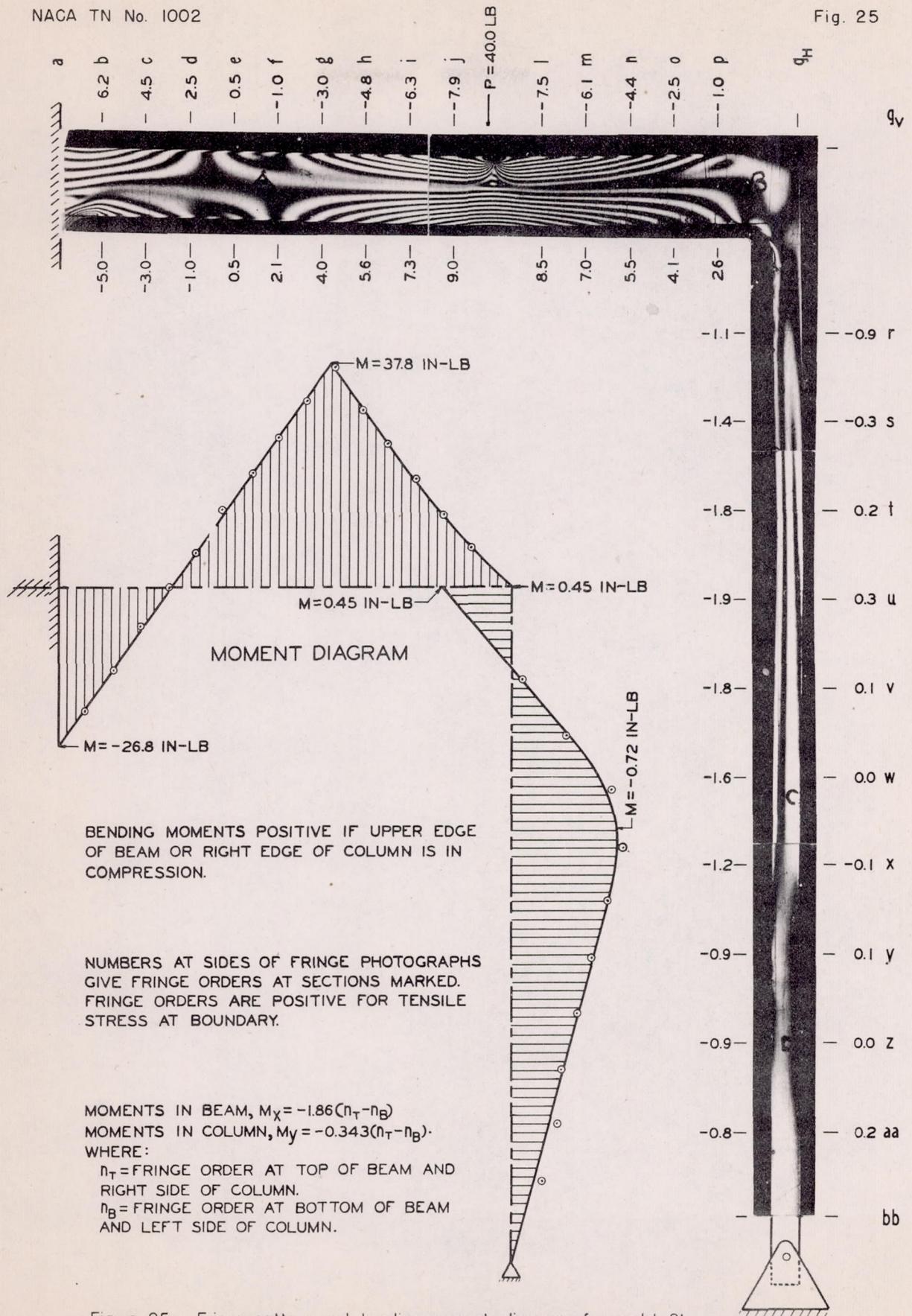n_B = FRINGE ORDER AT BOTTOM OF BEAM
AND LEFT SIDE OF COLUMN.

Figure 25.- Fringe pattern and bending moment diagrams for model 21,
P = 40 lb.

a   b   c   d   e   f   g   h   i   j   P = 75.0 LB   l   m   n   o   p   q_H

12.2   9.0   5.0   1.0   2.2   6.0   9.0   12.3   15.3   16.2   13.5   10.5   6.9   4.0

q_V

−11.0   −7.0   3.5   0.0   3.0   6.5   10.0   13.0   16.2   17.1   14.2   11.6   9.0   6.0

−3.2 −   − −1.8 r

−4.1 −   − −0.6 s

M = 73.8 IN-LB

−5.4 −   − 0.5 t

M = 1.0 IN-LB

M = 1.0 IN-LB

−6.2 −   − 1.2 u

MOMENT DIAGRAM

−6.6 −   − 1.6 v

M = −56.7 IN-LB

−6.7 −   − 1.6 w

BENDING MOMENTS POSITIVE IF UPPER EDGE
OF BEAM OR RIGHT EDGE OF COLUMN IS IN
COMPRESSION.

−6.7 −   − 1.5 x

M = −2.86 IN-LB

NUMBERS AT SIDES OF FRINGE PHOTOGRAPHS
GIVE FRINGE ORDERS AT SECTIONS MARKED.
FRINGE ORDERS ARE POSITIVE FOR TENSILE
STRESS AT BOUNDARY.

−5.3 −   − 0.1 y

−5.0 −   − −0.7 z

MOMENTS IN BEAM, $M_x = -1.86 (n_T - n_B)$.

MOMENTS IN COLUMN, $M_y = -0.343 (n_T - n_B)$.

WHERE:

   n_T = FRINGE ORDER AT TOP OF BEAM AND
   RIGHT SIDE OF COLUMN.

   n_B = FRINGE ORDER AT BOTTOM OF BEAM
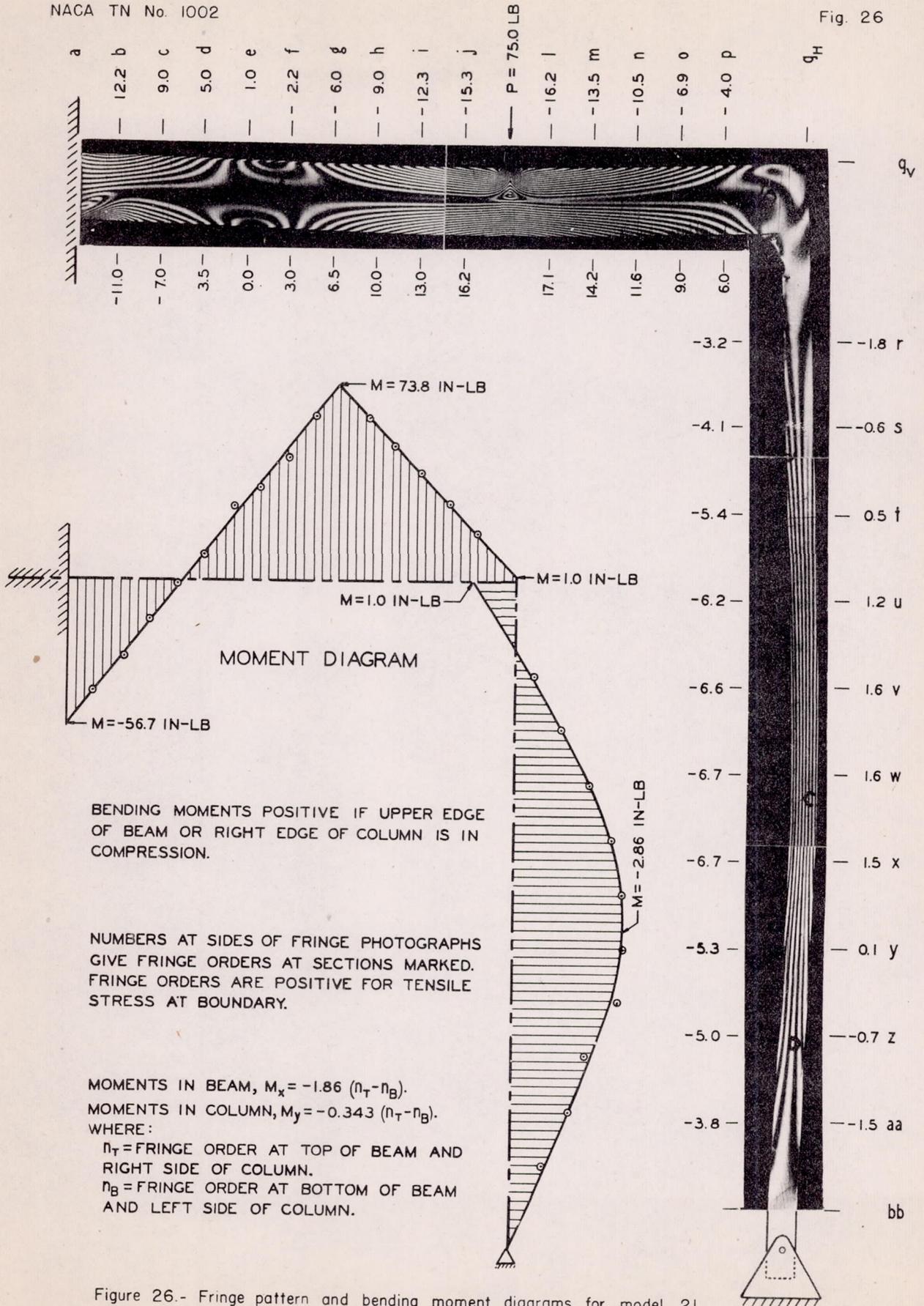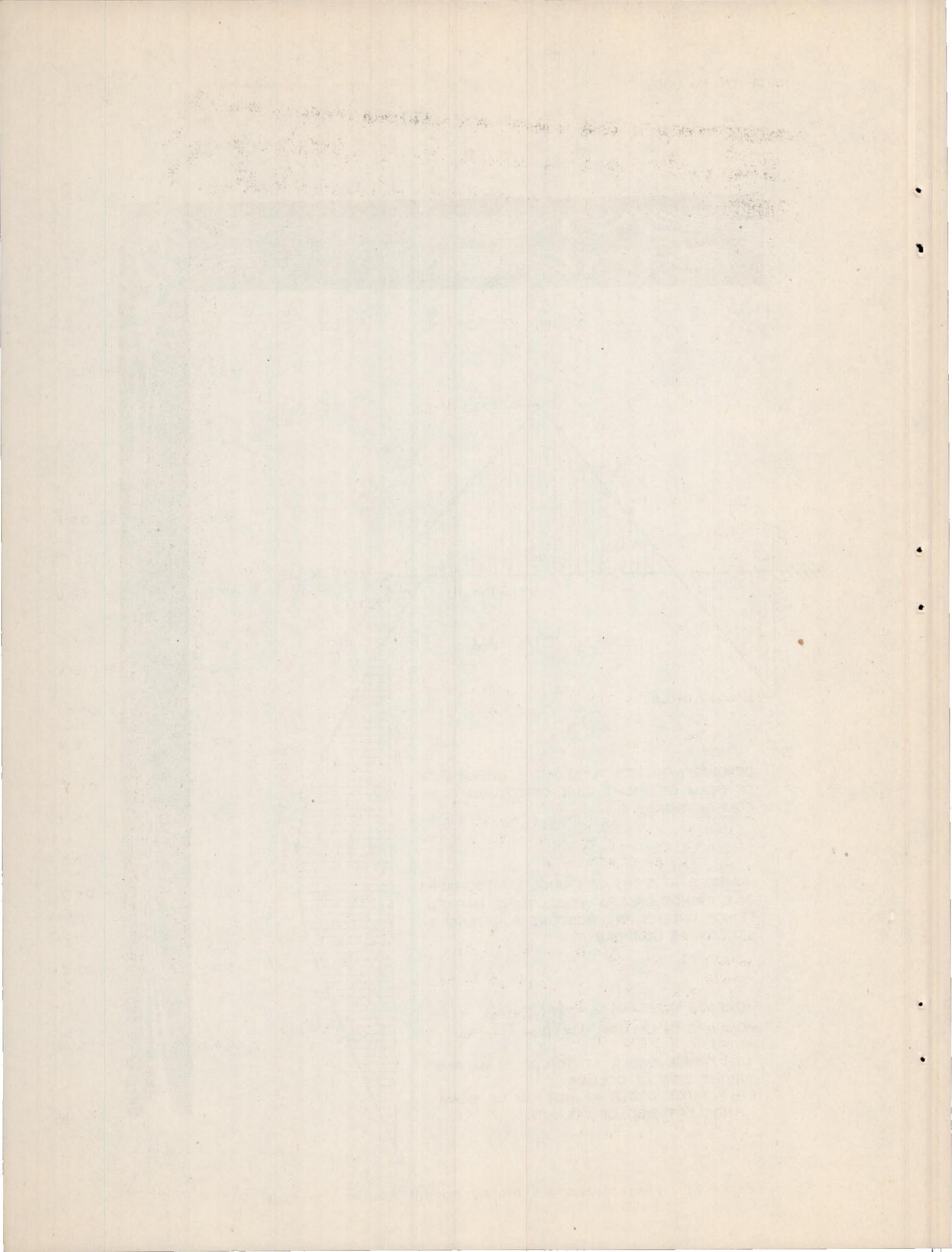   AND LEFT SIDE OF COLUMN.

−3.8 −   − −1.5 aa

bb

Figure 26.- Fringe pattern and bending moment diagrams for model 21,
     P = 75 lb.

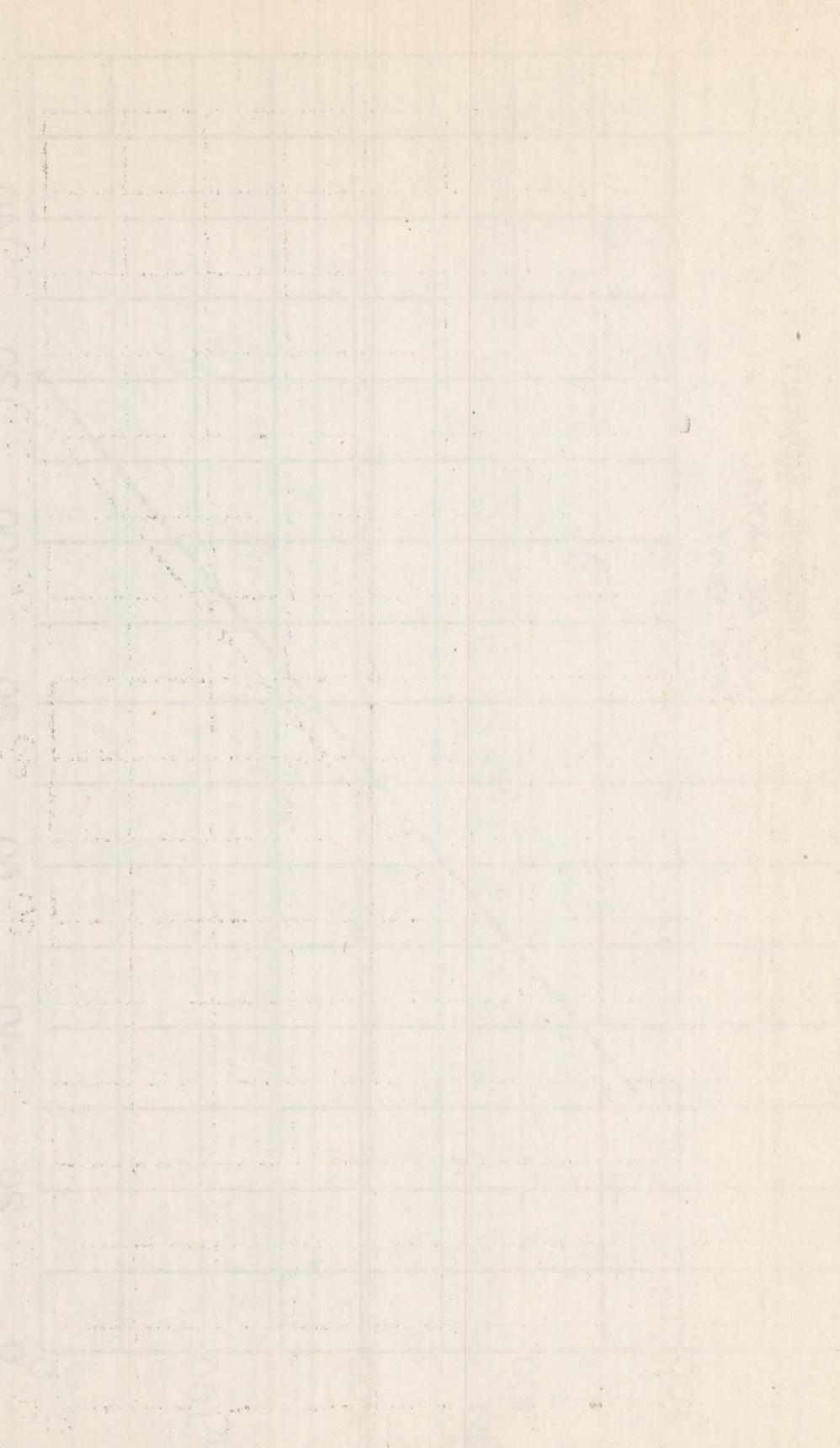M = BENDING MOMENT IN VERTICAL LEG OF MODEL 21 AT 3.80" FROM PIN JOINT

$$\frac{P\left(l_2 - \frac{h_1}{2}\right)}{M_C}$$
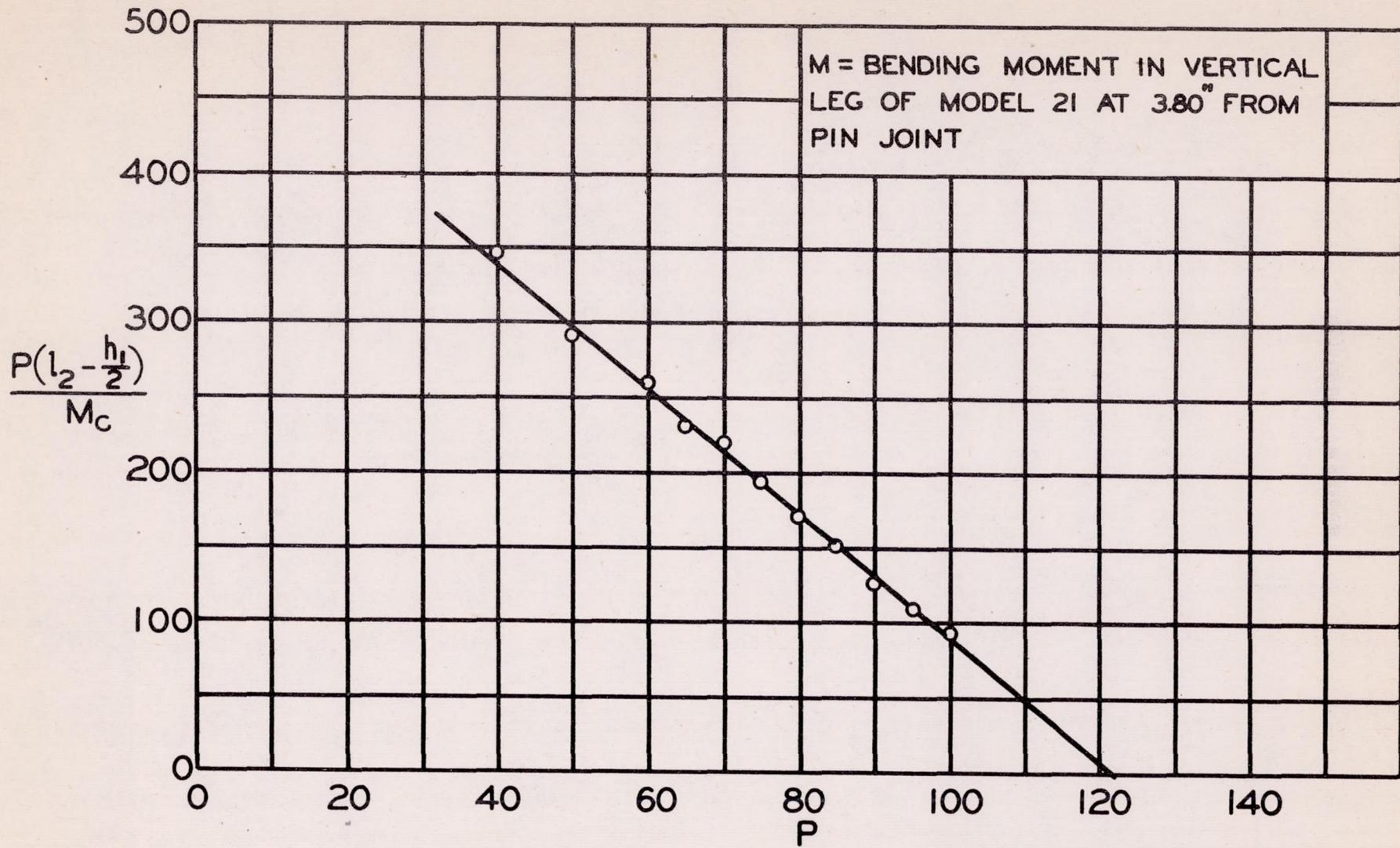
Figure 27.- Variation in bending moment, in vertical member of model 21, with load.

Fig. 27